Flow of charge and heat in thermal QCD within the weak magnetic field limit: A Bhatnagar-Gross-Krook model approach

Anowar Shaikh,[1,*] Shubhalaxmi Rath,[2,†] Sadhana Dash,[2,‡] and Binata Panda[1,§]

[1]*Department of Physics, Indian Institute of Technology (Indian School of Mines), Dhanbad, Jharkhand 826004, India*

[2]*Department of Physics, Indian Institute of Technology Bombay, Mumbai 400076, India*

(Received 6 December 2022; accepted 11 August 2023; published 26 September 2023)

We have computed the charge and heat transport coefficients of hot QCD matter by solving the relativistic Boltzmann transport equation using the Bhatnagar-Gross-Krook (BGK) model approximation with a modified collision integral in the weak magnetic-field regime. This modified collision integral enhances both charge and heat transport phenomena which can be understood by the large values of the above-mentioned coefficients in comparison to the relaxation collision integral. We have also presented a comparative study of coefficients like the electrical conductivity (σ_{el}), Hall conductivity (σ_H), thermal conductivity (κ), and Hall-type thermal conductivity (κ_H) in weak and strong magnetic fields in the BGK model approximation. The effects of weak magnetic field and finite chemical potential on the transport coefficients have been explored using a quasiparticle model. Moreover, we have also studied the effects of weak magnetic field and finite chemical potential on the Lorenz number, Knudsen number, specific heat, elliptic flow, and Wiedemann-Franz law.

DOI: 10.1103/PhysRevD.108.056021

I. INTRODUCTION

The possible existence of the deconfined state of quarks and gluons, known as quark gluon plasma (QGP) has been theoretically predicted by quantum chromodynamics (QCD). The creation of such a state has been achieved in the heavy-ion collision experiments at the Relativistic Heavy Ion Collider (RHIC) at BNL and the Large Hadron Collider (LHC) at CERN. In such collisions, strong magnetic fields are expected to be produced in the perpendicular direction to the collision plane. The strength of the magnetic field can be expressed in terms of the pion mass scale as $eB = m_\pi^2$ at RHIC [1] and $eB = 15m_\pi^2$ at LHC [2]. The creation of QGP in laboratory is of great phenomenological significance. The extensive understanding of various aspects of QGP in the presence of magnetic field is becoming increasingly relevant. In recent years, various properties of QGP in the presence of magnetic field have been studied by different research groups. Some of them are chiral magnetic effect [3,4], axial magnetic effect [5,6], magnetic and inverse magnetic catalysis [7,8], the nonlinear electromagnetic current [9,10], chiral vortical effect [11], the axial Hall current [12], refractive indices and decay constant [13,14], dispersion relation in magnetized thermal QED [15], photon and dilepton productions from QGP [16–18], thermodynamic and magnetic properties [19–22], heavy quark diffusion [23], thermoelectric responses of hot QCD medium in a time-varying magnetic field [24,25] and magnetohydrodynamics [26,27].

The transport coefficients like, electrical conductivity (σ_{el}) and thermal conductivity (κ) carry the information about the charge and heat transport in the medium, respectively. Electrical conductivity plays an important role for the study of chiral magnetic effects [3,4], emission rate of soft photons [28], etc. The effect of magnetic field on electrical conductivity has already been studied via different approaches, such as the dilute instanton-liquid model [29], the diagrammatic method using the real-time formalism [30], the quenched SU(2) lattice gauge theory [31], the effective fugacity approach [32], etc. Studies on the thermal conductivity of a hot QCD matter in a strong magnetic field have been done in Refs. [33,34]. In the literature, different approaches are available for computing these coefficients, such as the relativistic Boltzmann transport equation [35–38], the Chapman-Enskog approximation [39,40], the correlator technique using Green-Kubo formula [29,41,42], the quasiparticle model [43], etc.

*anowar.19dr0016@ap.iitism.ac.in
†shubhalaxmi@iitb.ac.in
‡sadhana@phy.iitb.ac.in
§binata@iitism.ac.in

Recently, in a work [44], the effects of weak magnetic field and finite chemical potential on the transport of charge and heat in a hot QCD matter have been studied by calculating the transport coefficients, such as the electrical conductivity (σ_{el}), the Hall conductivity (σ_H), the thermal conductivity (κ), and the Hall-type thermal conductivity (κ_H). The transport coefficients have been calculated by solving the relativistic Boltzmann transport equation in weak magnetic-field regime, and the complexities of the collision term were avoided by considering a mean-free path treatment in the kinetic theory approach within the relaxation time approximation (RTA). However, in such models, the charge is not conserved instantaneously, but only on an average basis over a cycle. This can be avoided by considering a modified collision term as introduced in the Bhatnagar-Gross-Krook (BGK) model [45]. The effects of this modified collision integral and strong magnetic field on charge and heat transport for hot QCD medium were recently explored in Ref. [46]. In BGK collisional kernel, the particle number is conserved instantaneously, and has been studied on plasma instabilities in Ref. [47]. Moreover, one can consider QGP as a system of massive noninteracting quasiparticles in the quasiparticle model framework [48,49]. For the study of QGP, this type of model is suitable as the medium formed in heavy-ion collision behaves like a strongly coupled system. Later, different research groups consider this model for different scenarios such as the Namb-Jona-Lasinio model [50–52], the thermodynamically consistent quasiparticle model [53,54], the quasiparticle model in a strong magnetic field [55,56], and the quasiparticle model with Gribov-Zwanziger quantization [57,58].

In this paper, we plan to explore the effects of weak magnetic field and finite chemical potential for a hot and dense QCD matter by estimating their respective response functions, viz. σ_{el}, σ_H, κ, and κ_H. A kinetic-theory approach with the BGK collision term in the relativistic Boltzmann transport equation has been used to calculate the above coefficients followed by the estimation of the Lorenz number, the Knudsen number, specific heat, the elliptic flow coefficient, etc. We also showed how these transport coefficients change as we shift to the quasiparticle description of partons, where the rest masses are replaced by the masses generated in the medium. A comparative discussion of the results with the previous two works [44,46] is also presented.

The rest of the paper has been organized as follows. Section II is dedicated to the calculation of charge and heat transport coefficients from the relativistic Boltzmann transport equation with a BGK collision integral in the weak magnetic-field regime. In Sec. III, we have discussed the results of these different kinds of conductivity, considering the rest mass of the quarks. The quasiparticle model is discussed in the weak magnetic field and finite chemical potential in Sec. IV A. The results of the above-stated transport coefficients are discussed in Sec. IV B. Section V describes various applications and their results obtained from these coefficients, such as the Lorenz number, the Knudsen number, specific heat, elliptic flow coefficient etc. Finally, Sec. VI summarizes the results.

A. Notations and conventions

Here the covariant derivative ∂_μ and $\partial_\mu^{(p)}$ are written for $\frac{\partial}{\partial x^\mu}$ and $\frac{\partial}{\partial p^\mu}$, respectively. The fluid four-velocity $u^\mu = (1,0,0,0)$ is normalized to unity in the rest frame ($u^\mu u_\mu = 1$). Throughout this paper, the subscript f stands for the flavor index with $f = u, d, s$. Moreover, q_f, g_f, and δf_f ($\delta\bar{f}_f$) are the electric charge, degeneracy factor and the infinitesimal change in the distribution function for the quark (antiquark) of the fth flavor, respectively. In Eq. (6), σ_0, σ_1, and σ_2 are the various components of the electrical conductivity tensor and $\mathbf{b} = \mathbf{B}/B$ indicates the direction of magnetic field. In Eq. (7), ϵ^{ij} denotes an antisymmetric 2×2 unit matrix. The Lorentz force is defined as $\mathbf{F} = q(\mathbf{E} + \mathbf{v}\times\mathbf{B})$ and the components of $F^{\mu\nu}$ are related to electric and magnetic fields as $F^{0i} = E^i$, $F^{i0} = -E^i$, and $F^{ij} = \frac{1}{2}\epsilon^{ijk}B_k$. Here m_f denotes the current quark mass (the values of m_f are 3 MeV, 5 MeV, and 100 MeV for up, down and strange quarks, respectively). In this work, $g_g = 2(N_c^2 - 1)$ represents the gluonic degrees of freedom, and $g_f(g_{\bar{f}}) = 2N_c$ denotes the quark (antiquark) degrees of freedom (for each flavor of quark), where $N_c = 3$ is the number of colors.

II. CHARGE AND HEAT TRANSPORT PROPERTIES OF A QCD MEDIUM IN THE PRESENCE OF MAGNETIC FIELD: A BGK MODEL APPROACH

The Boltzmann transport equation for a single particle distribution function is given by

$$\frac{\partial f_f}{\partial t} + \frac{\mathbf{p}}{m}.\nabla f_f + \mathbf{F}.\frac{\partial f_f}{\partial \mathbf{p}} = \left(\frac{\partial f_f}{\partial t}\right)_{\mathbf{c}} = \mathbf{C}[f_f], \quad (1)$$

where $\mathbf{F}$ is the force field acting on the particles in the medium and m is the mass of particle. The right-hand side term arises due to collisions between particles in the medium. The zero value of this term indicates a collisionless system referred to as the Vlasov equation. Even for the simplest solution for the above Eq. (1), one faces various difficulties because of the complicated nature of the collision term. The term $(\frac{\partial f_f}{\partial t})_c$ represents the instantaneous change in the distribution function due to the collisions between particles. In order to obtain a complete solution, we will start by discussing some mathematical models by which we can adequately treat the collision term.

In the case of relaxation time approximation, where the collision term is being replaced by a relaxation term having a form as given below,

$$\left(\frac{\partial f_f}{\partial t}\right)_c = -\frac{1}{\tau(p)}(f_f(x,p,t) - f_{\mathrm{eq},f}(p)), \qquad (2)$$

where we can write $f_f(x,p,t) = f_{\mathrm{eq},f}(p) + \delta f_f(x,p,t)$ and $\tau(p)$ signifies the relaxation time for occurring collisions which forge ahead the distribution function to the equilibrium state. In order to allow the linearization of the Boltzmann equation, we can assume the quark distribution function is close to equilibrium with a small deviation from equilibrium. Here the term $\frac{1}{\tau}$ acts as a damping frequency. The instantaneous conservation of charge appears to be an elementary issue of this model. To shed the crunch, the BGK model introduces a new type of collision kernel, which is given as

$$\left(\frac{\partial f_f}{\partial t}\right)_c = -\frac{1}{\tau(p)}\left(f_f(x,p,t) - \frac{n(x,t)}{n_{\mathrm{eq}}} f_{\mathrm{eq},f}(p)\right), \qquad (3)$$

where $n(x,t)$ is known as fluctuating density or perturbed density calculated as $\int f_f(x,p,t) d^3p$ which gives zero value after integrating over momenta, thus indicating instantaneous conservation of particle number during collisions in the system. Here we are considering the general relativistic covariant form of the Boltzmann transport equation for a medium of quarks and gluons given as

$$p^\mu \partial_\mu f_f + qF^{\mu\nu} p_\nu \partial_\mu^{(p)} f_f = C[f_f] = -\frac{p^\mu u_\mu}{\tau(p)} \times \left(f_f(x,p,t) - \frac{n(x,t)}{n_{\mathrm{eq}}} f_{\mathrm{eq},f}(p)\right), \qquad (4)$$

where $F^{\mu\nu}$ is the electromagnetic field strength tensor representing the external electric and magnetic fields applied to the system. We will now see in forthcoming sections how the above-mentioned collision integral affects the solution of the relativistic Boltzmann transport equation in the presence of a weak magnetic field. We also discuss the consequences on the transport of current and heat in terms of their respective transport coefficients, such as σ_{el}, σ_H, κ, and κ_H and the derived coefficients from them, namely the Lorenz number, the Knudsen number, elliptic flow, and specific heat. The two subsections of the present section are arranged as follows. We will begin with the formalism of electric charge transport and calculation of corresponding transport coefficients (σ_{el}, σ_H) within the weak magnetic-field regime in Sec. II A. Further, Sec. II B contains the formalism of heat transport phenomena and the calculation of associated transport coefficients (κ, κ_H) within the weak magnetic-field regime.

A. Charge transport properties: Electrical conductivity and Hall conductivity

In an attempt to see the effects of the magnetic field on the charge transport phenomena, we need to calculate the electric current density of the magnetized medium. When a thermal QCD medium containing quarks, antiquarks, and gluons of different flavors gets in contact with an external electric field, the medium gets infinitesimally disturbed. Due to this electric field, there is an induced current density in the medium, whose spatial component (J^i) is directly proportional to the electric field (E) with a proportionality constant, known as electrical conductivity (σ_{el}) and is given by

$$J^i = \sum_f g_f q_f \int \frac{d^3p}{(2\pi)^3} \frac{p^i}{\omega_f} [\delta f_f(x,p) + \delta \bar{f}_f(x,p)], \qquad (5)$$

where J^i represents the spatial part of the current density vector. At first, we have to calculate the nonequilibrium part of the distribution function from Eq. (4) to get the current density. In the presence of an electromagnetic field, the general form of spatial current density can be written as

$$J^i = \sigma^{ij} E_j = \sigma_0 \delta^{ij} E_j + \sigma_1 \epsilon^{ijk} b_k E_j + \sigma_2 b^i b^j E_j. \qquad (6)$$

Equation (6) can be rewritten in a case where the electric field and magnetic field are both perpendicular to each other as

$$J^i = \sigma^{ij} E_j = (\sigma_{el} \delta^{ij} + \sigma_H \epsilon^{ij}) E_j, \qquad (7)$$

where σ_0 and σ_1 denote electrical conductivity (σ_{el}) and Hall conductivity (σ_H), respectively. Now one can obtain the expressions for electrical conductivity and Hall conductivity with the help of Eqs. (5) and (7). In order to do that, we start with the relativistic Boltzmann transport equation (RBTE), i.e., Eq. (4), which can be rewritten as

$$p^\mu \frac{\partial f_f}{\partial x^\mu} + qF^{\mu\nu} p_\nu \frac{\partial f_f}{\partial p^\mu} = C[f_f] = -\frac{p_\mu u^\mu}{\tau_f}(f_f - n_f n_{\mathrm{eq},f}^{-1} f_{\mathrm{eq},f}), \qquad (8)$$

where τ_f is the relaxation time, i.e., the time required to bring the perturbed system back to its equilibrium state and $\nu_f = \frac{1}{\tau_f}$ indicates the collision frequency of the medium. The equilibrium distribution functions for fth flavor quark and antiquark are given as

$$f_{\mathrm{eq},f} = \frac{1}{e^{\beta(\omega_f - \mu_f)} + 1}, \qquad (9)$$

$$\bar{f}_{\mathrm{eq},f} = \frac{1}{e^{\beta(\omega_f + \mu_f)} + 1}, \qquad (10)$$

respectively, where $\omega_f = \sqrt{(\mathbf{p}^2 + m_f^2)}$, $\beta = \frac{1}{T}$, and μ_f represents the chemical potential of fth flavor quark. In a weak magnetic field regime, the temperature scale is more dominant than the magnetic field scale in equilibrium. For this reason, we neglect the effects of Landau quantization on phase space and scattering processes. The expression for τ_f is given [59] by

$$\tau_f(T) = \frac{1}{5.1T\alpha_s^2 \log(1/\alpha_s)[1 + 0.12(2N_f + 1)]}. \tag{11}$$

Here α_s is the QCD running coupling constant, which is a function of temperature, magnetic field and chemical potential, and it has the following [60] form,[1]

$$\alpha_s(\Lambda^2, eB) = \frac{\alpha_s(\Lambda^2)}{1 + b_1\alpha_s(\Lambda^2)\ln(\frac{\Lambda^2}{\Lambda^2+eB})}, \tag{12}$$

where

$$\alpha_s(\Lambda^2) = \frac{1}{b_1 \ln\left(\frac{\Lambda^2}{\Lambda^2_{\overline{\rm MS}}}\right)}, \tag{13}$$

with $b_1 = \frac{(11N_c-2N_f)}{12\pi}$, $\Lambda_{\overline{\rm MS}} = 0.176$ GeV and $\Lambda = 2\pi\sqrt{T^2 + \left(\frac{\mu_f^2}{\pi^2}\right)}$. In the collision term, n_f and $n_{{\rm eq},f}$ signify the perturbed density and equilibrium density, respectively for the $f^{\rm th}$ flavor with a degeneracy of g_f. Both can be calculated from the equations given below,

$$n_f = g_f \int \frac{d^3p}{(2\pi)^3}(f_{{\rm eq},f} + \delta f_f), \tag{14}$$

$$n_{{\rm eq},f} = g_f \int \frac{d^3p}{(2\pi)^3} f_{{\rm eq},f}. \tag{15}$$

The RBTE (8) can be rewritten as

$$\begin{aligned}&\frac{\partial f_f}{\partial t} + \mathbf{v}.\frac{\partial f_f}{\partial \mathbf{r}} + \frac{\mathbf{p}.\mathbf{F}}{p^0}\frac{\partial f_f}{\partial p^0} + \mathbf{F}.\frac{\partial f_f}{\partial \mathbf{p}} = C[f_f] \\ &= -\frac{p_\mu u^\mu}{\tau_f}(f_f - n_f n^{-1}_{{\rm eq},f} f_{{\rm eq},f}).\end{aligned} \tag{16}$$

Now we consider the distribution function to be spatially homogeneous and also in a steady-state condition, which gives us the freedom to neglect the first two terms by taking $\frac{\partial f_f}{\partial \mathbf{r}} = 0, \frac{\partial f_f}{\partial t} = 0$ and finally the above equation is reduced to

$$\mathbf{v}.\mathbf{F}\frac{\partial f_f}{\partial p^0} + \mathbf{F}.\frac{\partial f_f}{\partial \mathbf{p}} = C[f_f] = -\frac{p_\mu u^\mu}{\tau_f}(f_f - n_f n^{-1}_{{\rm eq},f} f_{{\rm eq},f}). \tag{17}$$

By taking electric and magnetic fields in a perpendicular direction to each other, i.e., electric field along x-direction ($\mathbf{E} = E\hat{x}$) and magnetic field along z-direction ($\mathbf{B} = B\hat{z}$), the above equation appears to be

$$\begin{aligned}&\tau_f qEv_x\frac{\partial f_f}{\partial p^0} + \tau_f qBv_y\frac{\partial f_f}{\partial p_x} - \tau_f qBv_x\frac{\partial f_f}{\partial p_y} \\ &= (n_f n^{-1}_{{\rm eq},f} f_{{\rm eq},f} - f_f).\end{aligned} \tag{18}$$

For a satisfactory solution to the above equation, we propose the following ansatz for the distribution function, which was first introduced in [42] and was later followed by various research groups [61–64],

$$f_f = n_f n^{-1}_{{\rm eq},f} f_{{\rm eq},f} - \tau_f q\mathbf{E}.\frac{\partial f_{{\rm eq},f}}{\partial \mathbf{p}} - \mathbf{\Gamma}.\frac{\partial f_{{\rm eq},f}}{\partial \mathbf{p}}, \tag{19}$$

where $\mathbf{\Gamma}$ is an unknown quantity which is constructed in such a way that it depends on both electric field and magnetic field in weak magnetic-field limit (it will be more evident in the forthcoming sections where we will obtain its expression). Neglecting higher-order terms of eB in Eq. (19), one can easily show that the unknown quantity $\mathbf{\Gamma}$ should be a function of eB. For weak magnetic-field regime, the magnetic field is not the dominant scale as compared to the temperature scale of the thermal medium in equilibrium. Thus, the effect of Landau quantization on the phase space and on the scattering processes have not been considered in the present work.[2]

Now with the help of an assumption that the quark distribution function is in the neighborhood of equilibrium, we can evaluate these quantities as follows:

$$\left.\begin{aligned}\frac{\partial f_{{\rm eq},f}}{\partial p_x} &= -\beta v_x f_{{\rm eq},f}(1 - f_{{\rm eq},f}) \\ \frac{\partial f_{{\rm eq},f}}{\partial p_y} &= -\beta v_y f_{{\rm eq},f}(1 - f_{{\rm eq},f}) \\ \frac{\partial f_{{\rm eq},f}}{\partial p_z} &= -\beta v_z f_{{\rm eq},f}(1 - f_{{\rm eq},f})\end{aligned}\right\}. \tag{20}$$

With the help of Eqs. (19) and (20) at high temperature, Eq. (18) can be simplified as

[1]We have taken the coupling constant from [60], where it has been calculated perturbatively in the weak magnetic-field limit with momentum transfer being larger than the magnetic field.

[2]Within BGK approximation in the strong magnetic field limit [46], the authors had considered the lowest Landau-level approximation in their study, as a result they used the modified dispersion relation, EOS and other modified quantities appropriate for the strong magnetic field regime.

$$\tau_f qEv_x\frac{\partial f_f}{\partial p^0}+\beta f_{\mathrm{eq},f}(\Gamma_x v_x+\Gamma_y v_y+\Gamma_z v_z)-qB\tau_f\left(v_x\frac{\partial f_f}{\partial p_y}-v_y\frac{\partial f_f}{\partial p_x}\right)=0. \tag{21}$$

Solving the above equation, we have[3]

$$\left.\begin{aligned}\Gamma_x=\tfrac{qE\tau_f(1-\omega_c^2\tau_f^2)}{(1+\omega_c^2\tau_f^2)}\\ \Gamma_y=-\tfrac{2qE\omega_c\tau_f^2}{(1+\omega_c^2\tau_f^2)}\\ \Gamma_z=0\end{aligned}\right\}. \tag{22}$$

Putting the values of Γ_x, Γ_y, and Γ_z in the ansatz, we get

$$(f_f-n_f n_{\mathrm{eq},f}^{-1}f_{\mathrm{eq},f})=2qE\beta v_x\left(\frac{\tau_f}{(1+\omega_c^2\tau_f^2)}\right)f_{\mathrm{eq},f}(1-f_{\mathrm{eq},f})-2qE\beta v_y\left(\frac{\omega_c\tau_f^2}{(1+\omega_c^2\tau_f^2)}\right)f_{\mathrm{eq},f}(1-f_{\mathrm{eq},f}). \tag{23}$$

One can reduce the left-hand side of Eq. (23) to[4]

$$(f_f-n_f n_{\mathrm{eq},f}^{-1}f_{\mathrm{eq},f})=\left[\delta f_f-g_f n_{\mathrm{eq},f}^{-1}f_{\mathrm{eq},f}\int_p\delta f_f\right]. \tag{24}$$

[5]Substituting the result of Eq. (24) in Eq. (23) we have

$$\delta f_f-g_f n_{\mathrm{eq},f}^{-1}f_{\mathrm{eq},f}\int_p\delta f_f=2qE\beta v_x\left(\frac{\tau_f}{(1+\omega_c^2\tau_f^2)}\right)f_{\mathrm{eq},f}(1-f_{\mathrm{eq},f})-2qE\beta v_y\left(\frac{\omega_c\tau_f^2}{(1+\omega_c^2\tau_f^2)}\right)f_{\mathrm{eq},f}(1-f_{\mathrm{eq},f}). \tag{25}$$

Neglecting higher-order terms ($(O(\delta f_f)^2)$), we get the solution of this equation as

$$\delta f_f=\left[\delta f_f^{(0)}+g_f n_{\mathrm{eq},f}^{-1}f_{\mathrm{eq},f}\int_{p\prime}\delta f_f^{(0)}\right], \tag{26}$$

where

$$\delta f_f^{(0)}=\left[2qE\beta v_x\left(\frac{\tau_f}{(1+\omega_c^2\tau_f^2)}\right)f_{\mathrm{eq},f}(1-f_{\mathrm{eq},f})-2qE\beta v_y\left(\frac{\omega_c\tau_f^2}{(1+\omega_c^2\tau_f^2)}\right)f_{\mathrm{eq},f}(1-f_{\mathrm{eq},f})\right]. \tag{27}$$

The infinitesimal change in the quark distribution function (δf_f) (see Appendix A) is obtained as

$$\begin{aligned}\delta f_f=&\left[2qE\beta v_x\left(\frac{\tau_f}{(1+\omega_c^2\tau_f^2)}\right)f_{\mathrm{eq},f}(1-f_{\mathrm{eq},f})-2qE\beta v_y\left(\frac{\omega_c\tau_f^2}{(1+\omega_c^2\tau_f^2)}\right)f_{\mathrm{eq},f}(1-f_{\mathrm{eq},f})\right]\\&+g_f n_{\mathrm{eq},f}^{-1}f_{\mathrm{eq},f}\int_{p\prime}\left[2qE\beta v_x\left(\frac{\tau_f}{(1+\omega_c^2\tau_f^2)}\right)f_{\mathrm{eq},f}(1-f_{\mathrm{eq},f})-2qE\beta v_y\left(\frac{\omega_c\tau_f^2}{(1+\omega_c^2\tau_f^2)}\right)f_{\mathrm{eq},f}(1-f_{\mathrm{eq},f})\right].\end{aligned} \tag{28}$$

Similarly, for antiquarks, we get

[3]Refer appendix A of Ref. [44] for detailed mathematical calculations.
[4]Refer appendix A of Ref. [46] for detailed mathematical calculations.
[5]Here we are using the symbol of momentum integration, $\int_p=\int d^3p/(2\pi)^3$.

$$\delta\bar{f}_f = \left[2\bar{q}E\beta v_x\left(\frac{\tau_{\bar{f}}}{(1+\omega_c^2\tau_{\bar{f}}^2)}\right)\bar{f}_{\mathrm{eq},f}(1-\bar{f}_{\mathrm{eq},f}) - 2\bar{q}E\beta v_y\left(\frac{\omega_c\tau_{\bar{f}}^2}{(1+\omega_c^2\tau_{\bar{f}}^2)}\right)\bar{f}_{\mathrm{eq},f}(1-\bar{f}_{\mathrm{eq},f})\right] + g_f n_{\mathrm{eq},f}^{-1}\bar{f}_{\mathrm{eq},f}$$
$$\times \int_{p\prime}\left[2\bar{q}E\beta v_x\left(\frac{\tau_{\bar{f}}}{(1+\omega_c^2\tau_{\bar{f}}^2)}\right)\bar{f}_{\mathrm{eq},f}(1-\bar{f}_{\mathrm{eq},f}) - 2\bar{q}E\beta v_y\left(\frac{\omega_c\tau_{\bar{f}}^2}{(1+\omega_c^2\tau_{\bar{f}}^2)}\right)\bar{f}_{\mathrm{eq},f}(1-\bar{f}_{\mathrm{eq},f})\right]. \tag{29}$$

Now, replacing the values of δf_f and $\delta\bar{f}_f$ in Eq. (5) and comparing it with Eq. (7), we get the final expressions for electrical conductivity and Hall conductivity under BGK model in weak magnetic field limit as

$$\sigma_{el}^{\mathrm{BGK}} = \frac{\beta}{3\pi^2}\sum_f g_f q_f^2 \int dp\,\frac{p^4}{\omega_f^2}\left[\left(\frac{\tau_f}{(1+\omega_c^2\tau_f^2)}\right)f_{\mathrm{eq},f}(1-f_{\mathrm{eq},f}) + \left(\frac{\tau_{\bar{f}}}{(1+\omega_c^2\tau_{\bar{f}}^2)}\right)\bar{f}_{\mathrm{eq},f}(1-\bar{f}_{\mathrm{eq},f})\right]$$
$$+ \frac{2\beta}{\sqrt{3}}\sum_f g_f^2 q_f^2 n_{\mathrm{eq},f}^{-1}\int_p \frac{p}{\omega_f} f_{\mathrm{eq},f}\int_{p\prime}\frac{p\prime}{\omega_f}\left[\left(\frac{\tau_f}{(1+\omega_c^2\tau_f^2)}\right)\right.$$
$$\left.\times f_{\mathrm{eq},f}(1-f_{\mathrm{eq},f}) + \left(\frac{\tau_{\bar{f}}}{(1+\omega_c^2\tau_{\bar{f}}^2)}\right)\bar{f}_{\mathrm{eq},f}(1-\bar{f}_{\mathrm{eq},f})\right], \tag{30}$$

$$\sigma_H^{\mathrm{BGK}} = \frac{\beta}{3\pi^2}\sum_f g_f q_f^2 \int dp\,\frac{p^4}{\omega_f^2}\left[\left(\frac{\omega_c\tau_f^2}{(1+\omega_c^2\tau_f^2)}\right)f_{\mathrm{eq},f}(1-f_{\mathrm{eq},f}) + \left(\frac{\omega_c\tau_{\bar{f}}^2}{(1+\omega_c^2\tau_{\bar{f}}^2)}\right)\bar{f}_{\mathrm{eq},f}(1-\bar{f}_{\mathrm{eq},f})\right]$$
$$+ \frac{2\beta}{\sqrt{3}}\sum_f g_f^2 q_f^2 n_{\mathrm{eq},f}^{-1}\int_p \frac{p}{\omega_f} f_{\mathrm{eq},f}\int_{p\prime}\frac{p\prime}{\omega_f}\left[\left(\frac{\omega_c\tau_f^2}{(1+\omega_c^2\tau_f^2)}\right)f_{\mathrm{eq},f}(1-f_{\mathrm{eq},f}) + \left(\frac{\omega_c\tau_{\bar{f}}^2}{(1+\omega_c^2\tau_{\bar{f}}^2)}\right)\bar{f}_{\mathrm{eq},f}(1-\bar{f}_{\mathrm{eq},f})\right]. \tag{31}$$

Expressions of $\sigma_{el}^{\mathrm{BGK}}$ [Eq. (30)] and σ_H^{BGK} [Eq. (31)] can be rewritten as

$$\sigma_{el}^{\mathrm{BGK}} = \sigma_{el}^{\mathrm{RTA}} + \sigma_{el}^{\mathrm{Corr}}, \tag{32}$$

$$\sigma_H^{\mathrm{BGK}} = \sigma_H^{\mathrm{RTA}} + \sigma_H^{\mathrm{Corr}}, \tag{33}$$

where

$$\sigma_{el}^{\mathrm{RTA}} = \frac{\beta}{3\pi^2}\sum_f g_f q_f^2 \int dp\,\frac{p^4}{\omega_f^2}\left[\left(\frac{\tau_f}{(1+\omega_c^2\tau_f^2)}\right)f_{\mathrm{eq},f}(1-f_{\mathrm{eq},f}) + \left(\frac{\tau_{\bar{f}}}{(1+\omega_c^2\tau_{\bar{f}}^2)}\right)\bar{f}_{\mathrm{eq},f}(1-\bar{f}_{\mathrm{eq},f})\right], \tag{34}$$

$$\sigma_{el}^{\mathrm{Corr}} = \frac{2\beta}{\sqrt{3}}\sum_f g_f^2 q_f^2 n_{\mathrm{eq},f}^{-1}\int_p \frac{p}{\omega_f} f_{\mathrm{eq},f}\int_{p\prime}\frac{p\prime}{\omega_f}\left[\left(\frac{\tau_f}{(1+\omega_c^2\tau_f^2)}\right)f_{\mathrm{eq},f}(1-f_{\mathrm{eq},f}) + \left(\frac{\tau_{\bar{f}}}{(1+\omega_c^2\tau_{\bar{f}}^2)}\right)\bar{f}_{\mathrm{eq},f}(1-\bar{f}_{\mathrm{eq},f})\right]. \tag{35}$$

Similarly,

$$\sigma_H^{\mathrm{RTA}} = \frac{\beta}{3\pi^2}\sum_f g_f q_f^2 \int dp\,\frac{p^4}{\omega_f^2}\left[\left(\frac{\omega_c\tau_f^2}{(1+\omega_c^2\tau_f^2)}\right)f_{\mathrm{eq},f}(1-f_{\mathrm{eq},f}) + \left(\frac{\omega_c\tau_{\bar{f}}^2}{(1+\omega_c^2\tau_{\bar{f}}^2)}\right)\bar{f}_{\mathrm{eq},f}(1-\bar{f}_{\mathrm{eq},f})\right], \tag{36}$$

$$\sigma_H^{\mathrm{Corr}} = \frac{2\beta}{\sqrt{3}}\sum_f g_f^2 q_f^2 n_{\mathrm{eq},f}^{-1}\int_p \frac{p}{\omega_f} f_{\mathrm{eq},f}\int_{p\prime}\frac{p\prime}{\omega_f}\left[\left(\frac{\omega_c\tau_f^2}{(1+\omega_c^2\tau_f^2)}\right)f_{\mathrm{eq},f}(1-f_{\mathrm{eq},f}) + \left(\frac{\omega_c\tau_{\bar{f}}^2}{(1+\omega_c^2\tau_{\bar{f}}^2)}\right)\bar{f}_{\mathrm{eq},f}(1-\bar{f}_{\mathrm{eq},f})\right]. \tag{37}$$

B. Heat transport properties: Thermal conductivity and Hall-type thermal conductivity

Heat flow in a system is defined as the difference between the energy flow and the enthalpy flow. It is directly proportional to the temperature gradient through a proportionality constant known as thermal conductivity. To study the heat transport in a medium, we need to calculate the thermal conductivity first. In four-vector notation, the heat flow is given by

$$Q_\mu = \Delta_{\mu\alpha}T^{\alpha\beta}u_\beta - h\Delta_{\mu\alpha}N^\alpha. \tag{38}$$

In the above equation, the projection operator ($\Delta_{\mu\alpha}$) and the enthalpy per particle (h) are respectively defined as

$$\Delta_{\mu\alpha} = g_{\mu\alpha} - u_\mu u_\alpha, \tag{39}$$

$$h = (\epsilon + P)/n, \tag{40}$$

where ϵ, P, and n represent the energy density, pressure, and particle number density, respectively, which are given by the following equations:

$$\epsilon = u_\alpha T^{\alpha\beta}u_\beta, \tag{41}$$

$$P = -\frac{\Delta_{\alpha\beta}T^{\alpha\beta}}{3}, \tag{42}$$

$$n = N^\alpha u_\alpha. \tag{43}$$

Here, the particle flow four-vector N^α and the energy-momentum tensor $T^{\alpha\beta}$ are defined as

$$N^\alpha = \sum_f g_f \int \frac{d^3p}{(2\pi)^3}\frac{p^\alpha}{\omega_f}[f_f(x,p) + \bar{f}_f(x,p)], \tag{44}$$

$$T^{\alpha\beta} = \sum_f g_f \int \frac{d^3p}{(2\pi)^3}\frac{p^\alpha p^\beta}{\omega_f}[f_f(x,p) + \bar{f}_f(x,p)]. \tag{45}$$

The spatial part of the heat flow four-vector is given by

$$Q^i = \sum_f g_f \int \frac{d^3p}{(2\pi)^3}\frac{p^i}{\omega_f}[(\omega_f - h_f)\delta f_f(x,p) + (\omega_f - h_{\bar{f}})\delta\bar{f}_f(x,p)], \tag{46}$$

where we use the fact that in the rest frame of the fluid, heat flow four-vector, and fluid four-vector are perpendicular to each other, i.e., $Q_\mu u^\mu = 0$ and the enthalpy per particle for the f^{th} flavor is given by

$$h_f = \frac{(\epsilon_f + P_f)}{n_{\text{eq},f}}, \tag{47}$$

where

$$\epsilon_f = g_f \int \frac{d^3p}{(2\pi)^3}\omega_f f_{\text{eq},f}, \tag{48}$$

$$P_f = \frac{g_f}{3}\int \frac{d^3p}{(2\pi)^3}\frac{p^2}{\omega_f}f_{\text{eq},f}. \tag{49}$$

In the Navier-Stokes equation, the heat flow is related to the gradients of temperature and pressure by

$$Q_\mu = \kappa\left[\nabla_\mu T - \frac{T}{(\epsilon + P)}\nabla_\mu P\right], \tag{50}$$

where κ represents the thermal conductivity for the medium and $\nabla_\mu = \partial_\mu - u_\mu u_\nu \partial^\nu$.

Now, the spatial component of the heat flow four-vector at finite magnetic field can be expressed [65] as

$$Q^i = -\kappa^{ij}\left[\partial_j T - \frac{T}{(\epsilon + P)}\partial_j P\right]. \tag{51}$$

Here, κ^{ij} represents the thermal conductivity tensor [65],

$$\kappa^{ij} = \kappa_0\delta^{ij} + \kappa_1\epsilon^{ijk}b_k + \kappa_2 b^i b^j. \tag{52}$$

In the above equation, κ_0, κ_1, and κ_2 are the various components of the thermal conductivity tensor. In this work, the gradients of temperature and pressure are taken perpendicular to the magnetic field, so the κ_2 term will vanish. Therefore, the above equation evolves to

$$Q^i = -(\kappa\delta^{ij} + \kappa_H\epsilon^{ij})\left[\partial_j T - \frac{T}{(n_{\text{eq},f}h_f)}\partial_j P\right]. \tag{53}$$

Here $\kappa_0 = \kappa$ and $\kappa_1 = \kappa_H$ are known as thermal conductivity and Hall-type thermal conductivity, respectively. One can find the expressions for κ and κ_H using Eqs. (46) and (53).

In order to calculate the infinitesimal change in the distribution function (δf_f), we start with the RBTE given in Eq. (8) with the help of Eq. (19),

$$\frac{\tau_f}{p^0}p^\mu\frac{\partial f_{\text{eq},f}}{\partial x^\mu} + \beta f_{\text{eq},f}(\Gamma_x v_x + \Gamma_y v_y + \Gamma_z v_z) + \tau_f qEv_x\frac{\partial f_f}{\partial p^0} - qB\tau_f\left(v_x\frac{\partial f_f}{\partial p_y} - v_y\frac{\partial f_f}{\partial p_x}\right) = 0. \tag{54}$$

Using Eq. (20) and considering $L = \frac{\tau_f}{p^0}p^\mu\frac{\partial f_{\text{eq},f}}{\partial x^\mu}$, Eq. (54) is reduced to

$$L - \beta f_{\text{eq},f}\tau_f qEv_x + \beta f_{\text{eq},f}(\Gamma_x v_x + \Gamma_y v_y + \Gamma_z v_z) - \frac{qB\tau_f\beta f_{\text{eq},f}}{\omega_f}(v_x\Gamma_y - v_y\Gamma_x) + \frac{\tau_f^2 q^2 BEv_y\beta f_{\text{eq},f}}{\omega_f} = 0. \tag{55}$$

Here L can be calculated as

$$L = \tau_f\beta f_{\text{eq},f}\frac{(\omega_f - h_f)}{T}v_x\left(\partial^x T - \frac{T}{nh_f}\partial^x P\right) + \tau_f\beta f_{\text{eq},f}\frac{(\omega_f - h_f)}{T}v_y\left(\partial^y T - \frac{T}{nh_f}\partial^y P\right) + \tau_f\beta f_{\text{eq},f} \times\left[p^0\frac{DT}{T} - \frac{p^\mu p^\alpha}{p^0}\nabla_\mu u_\alpha + TD\left(\frac{\mu_f}{T}\right)\right]. \tag{56}$$

Now, solving Eq. (55),[6] we get

$$\Gamma_x = qE\tau_f \frac{(1-\omega_c^2\tau_f^2)}{(1+\omega_c^2\tau_f^2)} - \frac{\tau_f}{(1+\omega_c^2\tau_f^2)}\frac{(\omega_f - h_f)}{T}\left(\partial^x T - \frac{T}{nh_f}\partial^x P\right) - \frac{\omega_c\tau_f^2}{(1+\omega_c^2\tau_f^2)}\frac{(\omega_f - h_f)}{T}\left(\partial^y T - \frac{T}{nh_f}\partial^y P\right), \tag{57}$$

$$\Gamma_y = -\frac{2qE\omega_c\tau_f^2}{(1+\omega_c^2\tau_f^2)} - \frac{\tau_f}{(1+\omega_c^2\tau_f^2)}\frac{(\omega_f - h_f)}{T}\left(\partial^y T - \frac{T}{nh_f}\partial^y P\right) + \frac{\omega_c\tau_f^2}{(1+\omega_c^2\tau_f^2)}\frac{(\omega_f - h_f)}{T}\left(\partial^x T - \frac{T}{nh_f}\partial^x P\right), \tag{58}$$

$$\Gamma_z = 0. \tag{59}$$

Putting the values of Γ_x, Γ_y, and Γ_z in Eq. (19), we get

$$\begin{aligned}(f_f - n_f n_{\mathrm{eq},f}^{-1} f_{\mathrm{eq},f}) = {}& \frac{2qE\tau_f v_x\beta}{(1+\omega_c^2\tau_f^2)} f_{\mathrm{eq},f}(1-f_{\mathrm{eq},f}) - \frac{2qE\omega_c\tau_f^2 v_y\beta}{(1+\omega_c^2\tau_f^2)} f_{\mathrm{eq},f}(1-f_{\mathrm{eq},f}) - \beta f_{\mathrm{eq},f}(1-f_{\mathrm{eq},f})\frac{\tau_f}{(1+\omega_c^2\tau_f^2)} \\ & \times \frac{(\omega_f - h_f)}{T}\left[v_x\left(\partial^x T - \frac{T}{nh_f}\partial^x P\right) + v_y\left(\partial^y T - \frac{T}{nh_f}\partial^y P\right)\right] - \beta f_{\mathrm{eq},f}(1-f_{\mathrm{eq},f})\frac{\omega_c\tau_f^2}{(1+\omega_c^2\tau_f^2)}\frac{(\omega_f - h_f)}{T} \\ & \times \left[v_x\left(\partial^y T - \frac{T}{nh_f}\partial^y P\right) - v_y\left(\partial^x T - \frac{T}{nh_f}\partial^x P\right)\right]. \end{aligned} \tag{60}$$

With the help of the same approach, we can reduce the left-hand side of the above Eq. (60) to obtain

$$\begin{aligned}\delta f_f - g_f n_{\mathrm{eq},f}^{-1} f_{\mathrm{eq},f}\int_p \delta f_f = {}& \frac{2qE\tau_f v_x\beta}{(1+\omega_c^2\tau_f^2)} f_{\mathrm{eq},f}(1-f_{\mathrm{eq},f}) - \frac{2qE\omega_c\tau_f^2 v_y\beta}{(1+\omega_c^2\tau_f^2)} f_{\mathrm{eq},f}(1-f_{\mathrm{eq},f}) - \beta f_{\mathrm{eq},f}(1-f_{\mathrm{eq},f})\frac{\tau_f}{(1+\omega_c^2\tau_f^2)} \\ & \times \frac{(\omega_f - h_f)}{T}\left[v_x\left(\partial^x T - \frac{T}{nh_f}\partial^x P\right) + v_y\left(\partial^y T - \frac{T}{nh_f}\partial^y P\right)\right] \\ & - \beta f_{\mathrm{eq},f}(1-f_{\mathrm{eq},f})\frac{\omega_c\tau_f^2}{(1+\omega_c^2\tau_f^2)}\frac{(\omega_f - h_f)}{T}\left[v_x\left(\partial^y T - \frac{T}{nh_f}\partial^y P\right) - v_y\left(\partial^x T - \frac{T}{nh_f}\partial^x P\right)\right]. \end{aligned} \tag{61}$$

After neglecting higher-order terms $(O(\delta f_f)^2)$, we get the solution of this equation as

$$\delta f_f = \delta f_f^{(0)} + g_f n_{\mathrm{eq},f}^{-1} f_{\mathrm{eq},f}\int_{p\prime} \delta f_f^{(0)}, \tag{62}$$

where

$$\begin{aligned}\delta f_f^{(0)} = {}& \frac{2qE\tau_f v_x\beta}{(1+\omega_c^2\tau_f^2)} f_{\mathrm{eq},f}(1-f_{\mathrm{eq},f}) - \frac{2qE\omega_c\tau_f^2 v_y\beta}{(1+\omega_c^2\tau_f^2)} f_{\mathrm{eq},f}(1-f_{\mathrm{eq},f}) - \beta f_{\mathrm{eq},f}(1-f_{\mathrm{eq},f})\frac{\tau_f}{(1+\omega_c^2\tau_f^2)}\frac{(\omega_f - h_f)}{T} \\ & \times \left[v_x\left(\partial^x T - \frac{T}{nh_f}\partial^x P\right) + v_y\left(\partial^y T - \frac{T}{nh_f}\partial^y P\right)\right] - \beta f_{\mathrm{eq},f}(1-f_{\mathrm{eq},f})\frac{\omega_c\tau_f^2}{(1+\omega_c^2\tau_f^2)}\frac{(\omega_f - h_f)}{T} \\ & \times \left[v_x\left(\partial^y T - \frac{T}{nh_f}\partial^y P\right) - v_y\left(\partial^x T - \frac{T}{nh_f}\partial^x P\right)\right]. \end{aligned} \tag{63}$$

So finally, we get the infinitesimal change in the quark distribution function (δf_f) (see Appendix B) as

[6]For detailed calculations, see Appendix B of Ref. [44].

$$\delta f_f = \frac{2qE\tau_f v_x\beta}{(1+\omega_c^2\tau_f^2)} f_{\mathrm{eq},f}(1-f_{\mathrm{eq},f}) - \frac{2qE\omega_c\tau_f^2 v_y\beta}{(1+\omega_c^2\tau_f^2)} f_{\mathrm{eq},f}(1-f_{\mathrm{eq},f}) - \beta f_{\mathrm{eq},f}(1-f_{\mathrm{eq},f})\frac{\tau_f}{(1+\omega_c^2\tau_f^2)}\frac{(\omega_f-h_f)}{T}$$
$$\times\left[v_x\left(\partial^x T-\frac{T}{nh_f}\partial^x P\right)+v_y\left(\partial^y T-\frac{T}{nh_f}\partial^y P\right)\right] - \beta f_{\mathrm{eq},f}(1-f_{\mathrm{eq},f})\frac{\omega_c\tau_f^2}{(1+\omega_c^2\tau_f^2)}\frac{(\omega_f-h_f)}{T}$$
$$\times\left[v_x\left(\partial^y T-\frac{T}{nh_f}\partial^y P\right)-v_y\left(\partial^x T-\frac{T}{nh_f}\partial^x P\right)\right] + g_f n_{\mathrm{eq},f}^{-1} f_{\mathrm{eq},f}\int_{p'}\left[\frac{2qE\tau_f v_x\beta}{(1+\omega_c^2\tau_f^2)} f_{\mathrm{eq},f}(1-f_{\mathrm{eq},f}) - \frac{2qE\omega_c\tau_f^2 v_y\beta}{(1+\omega_c^2\tau_f^2)}\right.$$
$$\times f_{\mathrm{eq},f}(1-f_{\mathrm{eq},f}) - \beta f_{\mathrm{eq},f}(1-f_{\mathrm{eq},f})\frac{\tau_f}{(1+\omega_c^2\tau_f^2)}\frac{(\omega_f-h_f)}{T}\left[v_x\left(\partial^x T-\frac{T}{nh_f}\partial^x P\right)+v_y\left(\partial^y T-\frac{T}{nh_f}\partial^y P\right)\right]$$
$$\left.-\beta f_{\mathrm{eq},f}(1-f_{\mathrm{eq},f})\frac{\omega_c\tau_f^2}{(1+\omega_c^2\tau_f^2)}\frac{(\omega_f-h_f)}{T}\left[v_x\left(\partial^y T-\frac{T}{nh_f}\partial^y P\right)-v_y\left(\partial^x T-\frac{T}{nh_f}\partial^x P\right)\right]\right]. \quad (64)$$

Similarly, for antiquarks, we get

$$\delta \bar{f}_f = \frac{2qE\tau_{\bar f} v_x\beta}{(1+\omega_c^2\tau_{\bar f}^2)} \bar f_{\mathrm{eq},f}(1-\bar f_{\mathrm{eq},f}) - \frac{2qE\omega_c\tau_{\bar f}^2 v_y\beta}{(1+\omega_c^2\tau_{\bar f}^2)} \bar f_{\mathrm{eq},f}(1-\bar f_{\mathrm{eq},f}) - \beta \bar f_{\mathrm{eq},f}(1-\bar f_{\mathrm{eq},f})\frac{\tau_{\bar f}}{(1+\omega_c^2\tau_{\bar f}^2)}\frac{(\omega_f-h_{\bar f})}{T}$$
$$\times\left[v_x\left(\partial^x T-\frac{T}{nh_f}\partial^x P\right)+v_y\left(\partial^y T-\frac{T}{nh_f}\partial^y P\right)\right] - \beta \bar f_{\mathrm{eq},f}(1-\bar f_{\mathrm{eq},f})\frac{\omega_c\tau_{\bar f}^2}{(1+\omega_c^2\tau_{\bar f}^2)}\frac{(\omega_f-h_{\bar f})}{T}$$
$$\times\left[v_x\left(\partial^y T-\frac{T}{nh_f}\partial^y P\right)-v_y\left(\partial^x T-\frac{T}{nh_f}\partial^x P\right)\right] + g_f n_{\mathrm{eq},f}^{-1} \bar f_{\mathrm{eq},f}\int_{p'}\left[\frac{2qE\tau_{\bar f} v_x\beta}{(1+\omega_c^2\tau_{\bar f}^2)} \bar f_{\mathrm{eq},f}(1-\bar f_{\mathrm{eq},f}) - \frac{2qE\omega_c\tau_{\bar f}^2 v_y\beta}{(1+\omega_c^2\tau_{\bar f}^2)}\right.$$
$$\times \bar f_{\mathrm{eq},f}(1-\bar f_{\mathrm{eq},f}) - \beta \bar f_{\mathrm{eq},f}(1-\bar f_{\mathrm{eq},f})\frac{\tau_{\bar f}}{(1+\omega_c^2\tau_{\bar f}^2)}\frac{(\omega_f-h_{\bar f})}{T}\left[v_x\left(\partial^x T-\frac{T}{nh_f}\partial^x P\right)+v_y\left(\partial^y T-\frac{T}{nh_f}\partial^y P\right)\right]$$
$$\left.-\beta \bar f_{\mathrm{eq},f}(1-\bar f_{\mathrm{eq},f})\frac{\omega_c\tau_{\bar f}^2}{(1+\omega_c^2\tau_{\bar f}^2)}\frac{(\omega_f-h_{\bar f})}{T}\left[v_x\left(\partial^y T-\frac{T}{nh_f}\partial^y P\right)-v_y\left(\partial^x T-\frac{T}{nh_f}\partial^x P\right)\right]\right]. \quad (65)$$

Now, replacing the values of δf_f and $\delta\bar f_f$ in Eq. (46) and comparing it with Eq. (53), we get the final expressions for thermal conductivity (κ^{BGK}) and Hall-type thermal conductivity (κ_H^{BGK}) under BGK model in weak magnetic field as

$$\kappa^{\mathrm{BGK}} = \frac{\beta^2}{6\pi^2}\sum_f g_f\int dp\,\frac{p^4}{\omega_f^2}\left[(\omega_f-h_f)^2\left(\frac{\tau_f}{1+\omega_c^2\tau_f^2}\right)f_{\mathrm{eq},f}(1-f_{\mathrm{eq},f}) + (\omega_f-h_{\bar f})^2\left(\frac{\tau_{\bar f}}{1+\omega_c^2\tau_{\bar f}^2}\right)\bar f_{\mathrm{eq},f}(1-\bar f_{\mathrm{eq},f})\right]$$
$$+\frac{\beta^2}{\sqrt{3}}\sum_f g_f^2 n_{\mathrm{eq},f}^{-1}\int_p \frac{p}{\omega_f}(\omega_f-h_f)f_{\mathrm{eq},f}\int_{p'}\frac{p'}{\omega_f}\left[(\omega_f-h_f)\left(\frac{\tau_f}{1+\omega_c^2\tau_f^2}\right)f_{\mathrm{eq},f}(1-f_{\mathrm{eq},f}) + (\omega_f-h_{\bar f})\right.$$
$$\left.\times\left(\frac{\tau_{\bar f}}{1+\omega_c^2\tau_{\bar f}^2}\right)\bar f_{\mathrm{eq},f}(1-\bar f_{\mathrm{eq},f})\right], \quad (66)$$

$$\kappa_H^{\mathrm{BGK}} = \frac{\beta^2}{6\pi^2}\sum_f g_f\int dp\,\frac{p^4}{\omega_f^2}\left[(\omega_f-h_f)^2\left(\frac{\omega_c\tau_f^2}{1+\omega_c^2\tau_f^2}\right)f_{\mathrm{eq},f}(1-f_{\mathrm{eq},f}) + (\omega_f-h_{\bar f})^2\left(\frac{\omega_c\tau_{\bar f}^2}{1+\omega_c^2\tau_{\bar f}^2}\right)\bar f_{\mathrm{eq},f}(1-\bar f_{\mathrm{eq},f})\right]$$
$$+\frac{\beta^2}{\sqrt{3}}\sum_f g_f^2 n_{\mathrm{eq},f}^{-1}\int_p \frac{p}{\omega_f}(\omega_f-h_f)f_{\mathrm{eq},f}\int_{p'}\frac{p'}{\omega_f}\left[(\omega_f-h_f)\left(\frac{\omega_c\tau_f^2}{1+\omega_c^2\tau_f^2}\right)f_{\mathrm{eq},f}(1-f_{\mathrm{eq},f})\right.$$
$$\left.+(\omega_f-h_{\bar f})\left(\frac{\omega_c\tau_{\bar f}^2}{1+\omega_c^2\tau_{\bar f}^2}\right)\bar f_{\mathrm{eq},f}(1-\bar f_{\mathrm{eq},f})\right]. \quad (67)$$

Here, we can write the expressions of κ^{BGK} and κ_H^{BGK} as an addition of two terms as

$$\kappa^{\rm BGK} = \kappa^{\rm RTA} + \kappa^{\rm Corr}, \tag{68}$$

$$\kappa_H^{\rm BGK} = \kappa_H^{\rm RTA} + \kappa_H^{\rm Corr}, \tag{69}$$

where

$$\kappa^{\rm RTA} = \frac{\beta^2}{6\pi^2}\sum_f g_f \int dp\,\frac{p^4}{\omega_f^2}\left[(\omega_f - h_f)^2\left(\frac{\tau_f}{1+\omega_c^2\tau_f^2}\right)f_{{\rm eq},f}(1-f_{{\rm eq},f}) + (\omega_f - h_{\bar f})^2\left(\frac{\tau_{\bar f}}{1+\omega_c^2\tau_{\bar f}^2}\right)\bar f_{{\rm eq},f}(1-\bar f_{{\rm eq},f})\right], \tag{70}$$

$$\begin{aligned}\kappa^{\rm corr} = \frac{\beta^2}{\sqrt{3}}\sum_f g_f^2 n_{{\rm eq},f}^{-1}\int_p \frac{p}{\omega_f}(\omega_f - h_f)f_{{\rm eq},f}\int_{p\prime}\frac{p\prime}{\omega_f}\Bigg[&(\omega_f - h_f)\left(\frac{\tau_f}{1+\omega_c^2\tau_f^2}\right)f_{{\rm eq},f}(1-f_{{\rm eq},f})\\ &+ (\omega_f - h_{\bar f})\left(\frac{\tau_{\bar f}}{1+\omega_c^2\tau_{\bar f}^2}\right)\bar f_{{\rm eq},f}(1-\bar f_{{\rm eq},f})\Bigg],\end{aligned} \tag{71}$$

$$\kappa_H^{\rm RTA} = \frac{\beta^2}{6\pi^2}\sum_f g_f \int dp\,\frac{p^4}{\omega_f^2}\left[(\omega_f - h_f)^2\left(\frac{\omega_c\tau_f^2}{1+\omega_c^2\tau_f^2}\right)f_{{\rm eq},f}(1-f_{{\rm eq},f}) + (\omega_f - h_{\bar f})^2\left(\frac{\omega_c\tau_{\bar f}^2}{1+\omega_c^2\tau_{\bar f}^2}\right)\bar f_{{\rm eq},f}(1-\bar f_{{\rm eq},f})\right], \tag{72}$$

$$\begin{aligned}\kappa_H^{\rm Corr} = \frac{\beta^2}{\sqrt{3}}\sum_f g_f^2 n_{{\rm eq},f}^{-1}\int_p \frac{p}{\omega_f}(\omega_f - h_f)f_{{\rm eq},f}\int_{p\prime}\frac{p\prime}{\omega_f}\Bigg[&(\omega_f - h_f)\left(\frac{\omega_c\tau_f^2}{1+\omega_c^2\tau_f^2}\right)f_{{\rm eq},f}(1-f_{{\rm eq},f})\\ &+ (\omega_f - h_{\bar f})\left(\frac{\omega_c\tau_{\bar f}^2}{1+\omega_c^2\tau_{\bar f}^2}\right)\bar f_{{\rm eq},f}(1-\bar f_{{\rm eq},f})\Bigg].\end{aligned} \tag{73}$$

III. RESULTS AND DISCUSSIONS

The charge transport coefficients (σ_{el}, σ_H) and heat transport coefficients (κ, κ_H) are estimated in the presence of weak magnetic field within the framework of the BGK model by considering the current masses of the quarks.

Figures 1 and 2 show the variations of σ_{el} and σ_H as functions of temperature, respectively. In Fig. 1(a), the BGK model estimations are compared with the RTA model results in the weak magnetic-field regime. It is found that due to this new BGK collision term, there is an increment in the charge transport phenomenon for the QCD medium.

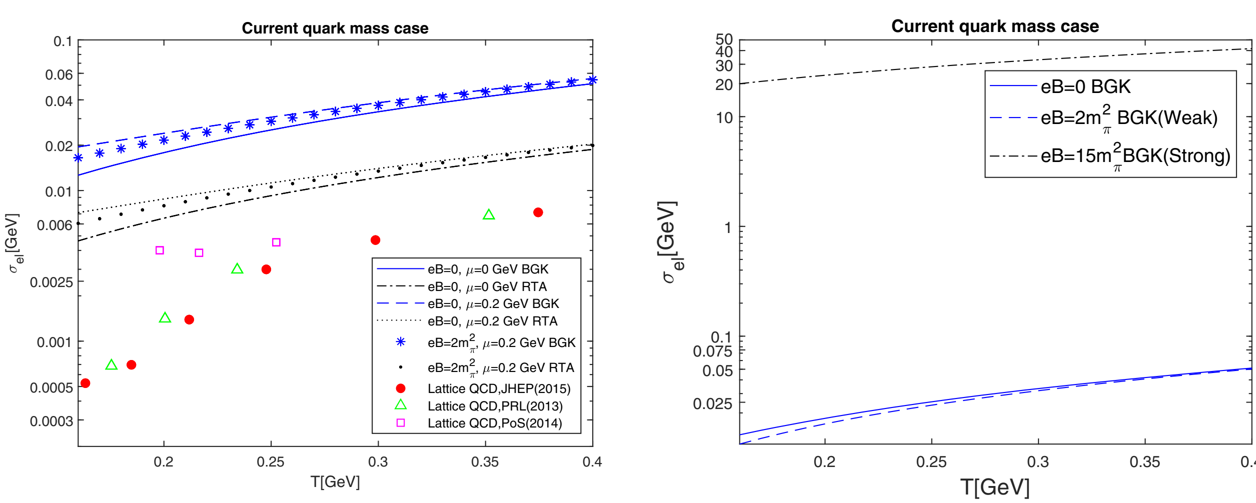

(a) (b)

FIG. 1. The variation of the electrical conductivity (σ_{el}) with temperature, (a) comparison with RTA model result (weak magnetic field) and (b) comparison with BGK model result (strong magnetic field).

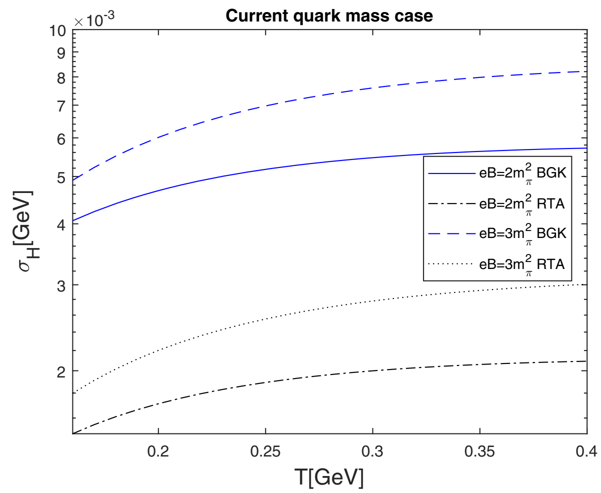

(a)

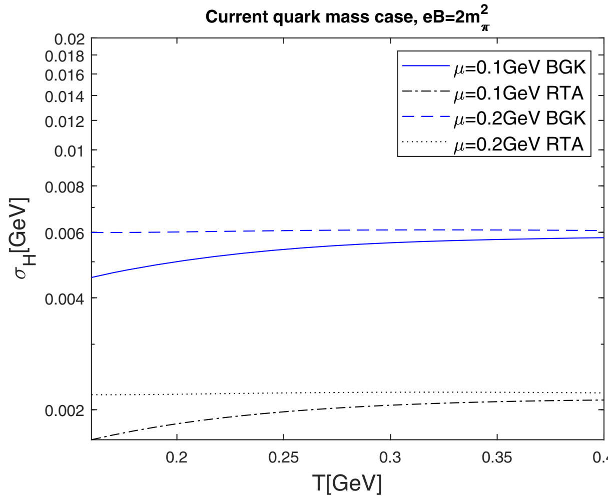

(b)

FIG. 2. The variation of the Hall conductivity (σ_H) with temperature, (a) comparison with RTA model result in the presence of weak magnetic field and (b) comparison with RTA model result in the presence of finite chemical potential.

This is indicated by the large value of electrical conductivity. The ratio of $\sigma_{el}^{\mathrm{BGK}}/\sigma_{el}^{\mathrm{RTA}}$ comes out to be 2.72. In Fig. 1(b), similar kind of comparison has been done with BGK model results for the strong magnetic field and it is observed that the weak magnetic field slightly reduces the electrical conductivity, contrary to the enhancement of the same by the strong magnetic field. We have compared the BGK model estimations in weak magnetic-field limit with the corresponding results of Ref. [46] in the strong magnetic field limit.[7] The large value of σ_{el} in Fig. 1(b) in the strong magnetic-field regime arises due to the large relaxation time, as it is inversely proportional to the square of the mass [Eq. (60) of Ref. [46]], where the current quark mass is very small. Similar results have been found in Ref. [30], where σ_{el} has been calculated in the diagrammatic method in the strong magnetic-field regime and its large value is attributed to the smaller value of the current quark masses.

We have also compared our results on the electrical conductivity with that of lattice QCD. In Fig. 1(a), it is observed that, with respect to the BGK model, σ_{el} in RTA model is nearer to the lattice results [66–68]. Specifically the lattice results in Refs. [66,67], which are obtained with the lattice simulations containing $2+1$ dynamical flavors on anisotropic lattices using spectral functions from correlators of the conserved vector current and using a tadpole-improved Clover action, respectively, report an increasing trend of σ_{el} up to temperature $T \simeq 0.26$ GeV and the slope gradually decreases at higher temperatures. A very small variation in σ_{el} with temperature is noticed in Ref. [68], which is calculated using the nonperturbatively improved clover Wilson valence quarks. The value of σ_{el} as estimated in Ref. [68] lies slightly below the RTA result, specifically at low temperatures. On the other hand, lattice results in Refs. [66,67] are comparable to our results at high temperatures. From the above discussion, it is inferred that the BGK model results are not at par with the lattice calculations.

In Fig. 2, we have done a suchlike comparison of our estimated results on Hall conductivity (σ_H). As presented in Fig. 2(a), it is found that the Hall conductivity shows increasing behavior with temperature for both RTA and BGK models at very small or zero chemical potential, which is attributed to the increase of distribution function with temperature. Conversely, Fig. 2(b) shows slight decreasing behavior of σ_H with temperature at finite chemical potential, which can be understood from the fact that, at finite μ, the increase of distribution function with T becomes smaller and the factor $\beta\tau_f^2$ ($\approx \frac{1}{T^3}$ in the weak magnetic-field case) appearing in the expression of Hall conductivity dominates, thus giving an overall decreasing effect to σ_H with increasing temperature. As compared to the RTA model result, the BGK model result on σ_H is larger. But in all cases, the magnitude of σ_H gets increased as the magnetic field increases, which is mainly due to the fact that the σ_H directly depends on the cyclotron frequency. At finite μ, the increase in σ_H is inferred from the increase of the net Hall current with the enhancement of the difference between the numbers of particles and antiparticles.

Figures 3 and 4 show the variations of κ and κ_H as functions of temperature, respectively. To be more specific, Figs. 3(a) and 3(b) represent the comparison of our estimated results of thermal conductivity (κ) with RTA model results of weak magnetic field and BGK model

[7] We have used the published results of Ref. [46] within BGK approximation in the strong magnetic-field regime for the comparison with our results in BGK approximation within the weak magnetic-field regime.

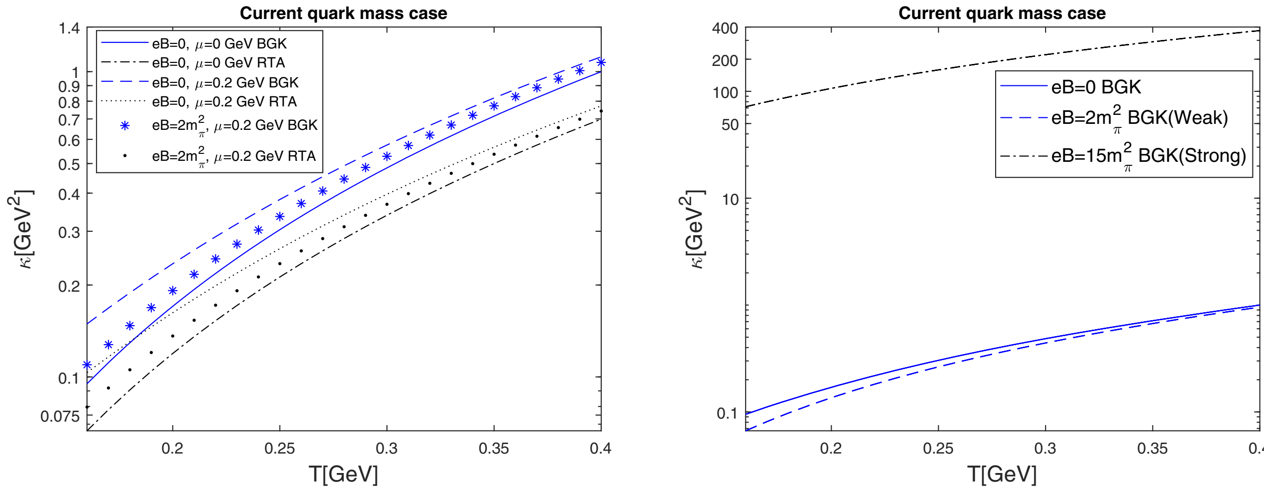

(a) (b)

FIG. 3. The variation of the thermal conductivity (κ) with temperature, (a) comparison with RTA model result (weak magnetic field). and (b) comparison with BGK model result (strong magnetic field).

results of strong magnetic field, respectively, whereas Figs. 4(a) and 4(b) show the comparison of our calculated results of κ_H with RTA model results for weak magnetic field and for finite chemical potential, respectively. The ratio of $\kappa^{\mathrm{BGK}}/\kappa^{\mathrm{RTA}}$ comes out to be 1.42. Thus, the above discussions imply that our collision integral is more sensitive to charge transport than heat transport.

Like the RTA model, in BGK model also, κ_H is directly associated with the cyclotron frequency in contrast to κ, so the magnitude of κ_H gets increased with the magnetic field even in the weak magnetic-field regime. The emergence of finite chemical potential also helps in enhancing the magnitude of κ_H. It is observed that both κ and κ_H increase with T, but a reverse effect of T on these conductivities is expected due to the presence of terms $\beta^2\tau_f$ and $\beta^2\tau_f^2$ in the expressions of κ and κ_H, respectively, but the increase of enthalpy per particle and the increase of distribution function with temperature reduce this reverse effect and give an increasing effect to κ and κ_H with temperature.

IV. QUASIPARTICLE MODEL (QPM) AND THE TRANSPORT COEFFICIENTS

A. Quasiparticle description of QGP

Noninteracting quasiparticles in a thermal medium obtain some masses due to the interaction with the medium, which are known as thermal masses. In the present context, we can consider QGP as a system of massive noninteracting quasiparticles in the quasiparticle model framework. This quasiparticle quark-gluon plasma (qQGP) model is widely

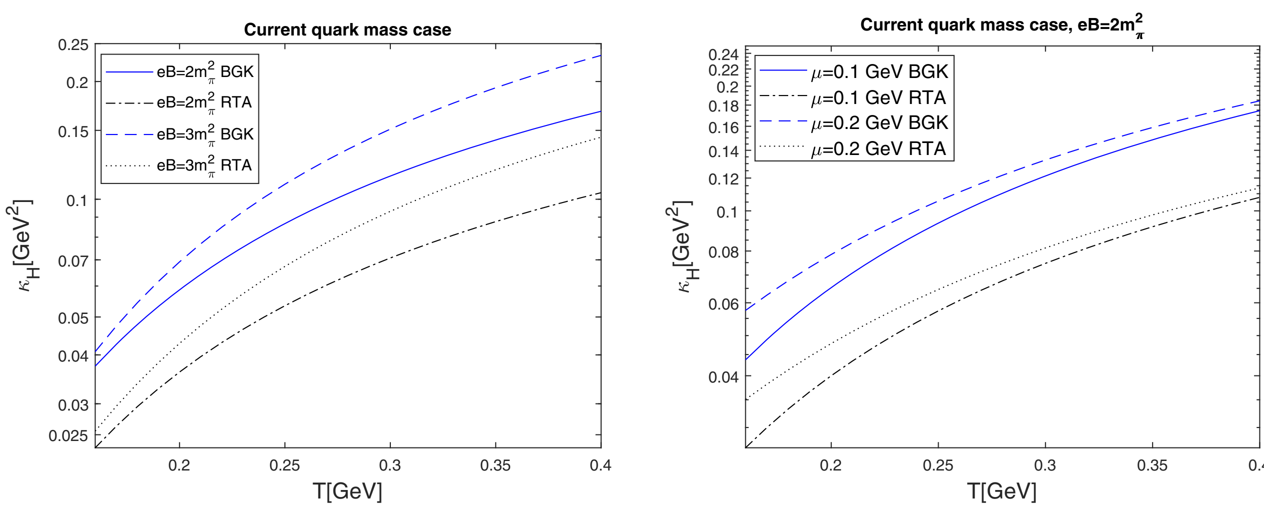

(a) (b)

FIG. 4. The variation of the Hall-type thermal conductivity (κ_H) with temperature, (a) comparison with RTA model result in the presence of weak magnetic field and (b) comparison with RTA model result in the presence of finite chemical potential.

used to describe the nonideal behavior of QGP. In the case of a pure thermal medium, the quasiparticle masses of particles depend only on the temperature of the medium, but for a dense thermal medium, they also depend on chemical potential. The thermal mass (squared) of quark for a dense QCD medium is given [69,70] by

$$m_{fT}^2 = \frac{g^2T^2}{6}\left(1+\frac{\mu_f^2}{\pi^2T^2}\right), \tag{74}$$

with $g = (4\pi\alpha_s)^{1/2}$, where the expression of α_s is given in Eq. (12). It can be seen from Eq. (12) that α_s depends on temperature, chemical potential and magnetic field, which indicates that, it is not a fixed value, rather, its value changes depending on the values of T, eB, and μ_f and thus the value of the thermal mass changes accordingly. Here, the chemical potentials for all the three quarks are set to be the same ($\mu_f = \mu$).

The thermal quark mass used has been obtained from high temperature perturbative QCD calculations using the hard thermal-loop approximation, where higher-order coupling terms have been truncated [28,69,71]. The coupling g ($\sqrt{4\pi\alpha_s}$) used in this work is the extension of the pure T-dependent coupling to the T, eB-dependent coupling in the perturbative domain with temperature scale being larger than the magnetic field scale [60].

For a thermal QCD medium in the absence of magnetic field, the available energy scales are associated with the temperature and the quark mass. In the QGP phase consisting of light quarks and gluons, the temperature is large enough to become the highest-energy scale. In this high-temperature regime, the divergences encountered in the calculation of QCD thermodynamic observables, transport coefficients, and amplitudes are treated by applying the effective theories, one of which is the hard thermal loop (HTL) perturbation theory. In this theory, the loop momentum is of the order of T, i.e., the hard scale and the next scale is the soft scale of the order of gT (g is the coupling constant). When the thermal medium is exposed to a magnetic field, $\sqrt{eB}$ emerges as the new energy scale of the system in addition to T. Depending on the strength of magnetic field with respect to the temperature, the thermal medium may be considered as weakly magnetized or strongly magnetized. In particular, for a weakly magnetized thermal medium where $\sqrt{eB} \ll T$, T plays the role of largest energy scale. Therefore, one can in principle use the same resummation technique (HTL perturbation theory) to alleviate the divergences as done previously for the pure thermal medium. As a result, there is no violation of self-consistency in using $g(T)$ in place of $g(T, eB)$ (in the weak magnetic-field limit) in the thermal masses of partons.

Due to the temperature-dependent masses, there is a significant change in the transport phenomena of the given system and also in the corresponding transport coefficients. In the following section, our aim is to study the variations of electrical, Hall, thermal and Hall-type thermal conductivities with temperature considering the quasiparticle masses of the quarks. We also intend to compare our results in "BGK (weak)" with that in "BGK (strong)" [46]. As compared to the thermal mass in Eq. (74), the thermal mass [Eq. (109) in Ref. [46]] in "BGK (strong)" has a different form as it was calculated in the strong magnetic field limit ($\sqrt{eB} \gg T$). In addition, weak and strong magnetic-field values are used for "BGK (weak)" and "BGK (strong)" cases, respectively. This comparison is helpful to understand the behavior and properties of aforesaid transport coefficients in different regimes (the weak and the strong magnetic-field regimes) within the BGK model.

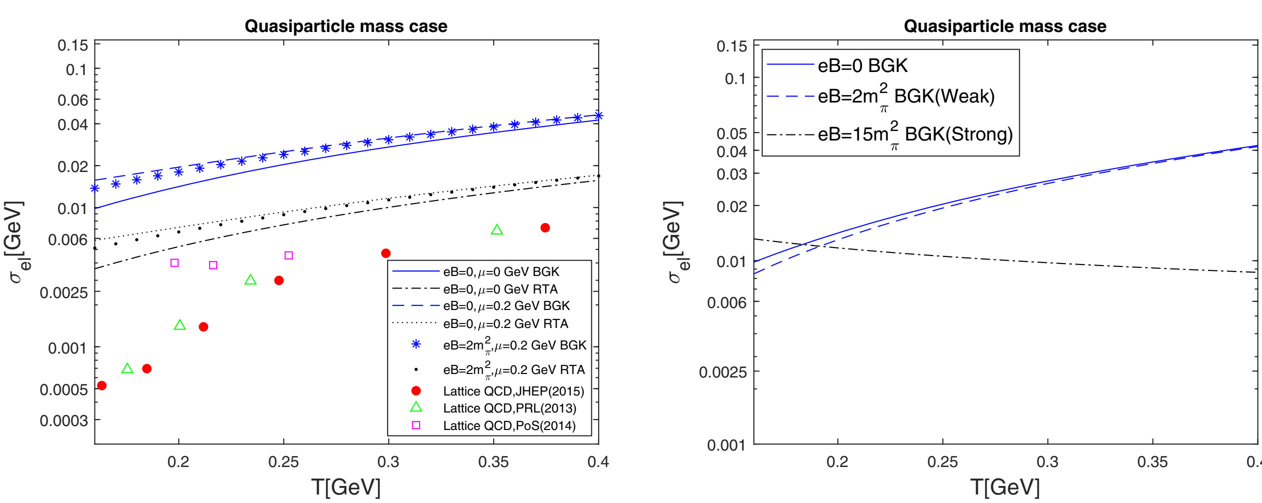

(a) (b)

FIG. 5. The variation of the electrical conductivity (σ_{el}) with temperature, (a) comparison with RTA model result (weak magnetic field), and (b) comparison with BGK model result (strong magnetic field).

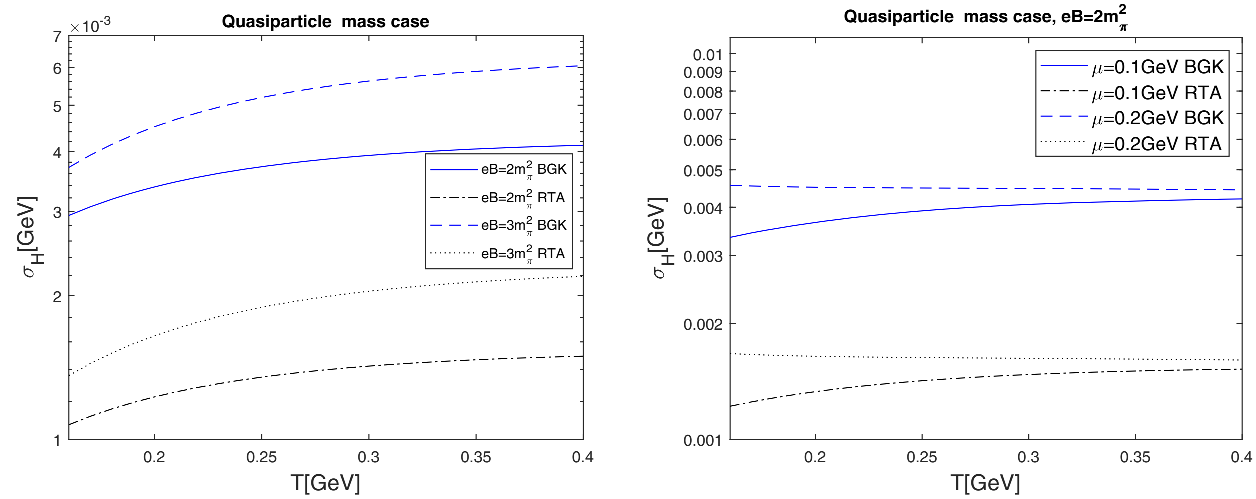

(a) (b)

FIG. 6. The variation of the Hall conductivity (σ_H) with temperature, (a) comparison with RTA model result in the presence of weak magnetic field and (b) comparison with RTA model result in the presence of finite chemical potential.

B. Results and discussions

In this section, the charge and thermal coefficients are reinvestigated with the thermal mass as given by Eq. (74). Figures 5 and 6 show the variations of σ_{el} and σ_H with temperature, respectively. To be more specific, in Figs. 5(a) and 5(b), we compare our results of electrical conductivity with the results of the RTA model (weak magnetic field) and BGK model (strong magnetic field). Similarly, Figs. 6(a) and 6(b) represent the comparison of Hall conductivity with the results of the RTA model in weak magnetic field and finite chemical potential, respectively. In Figs. 7 and 8, same comparisons have been done for κ and κ_H, respectively. In kinetic theory, all the transport coefficients depend on the distribution functions of partons in the medium. The distribution functions are observed to be slightly modified due to the quasiparticle masses of partons, which further causes change in the transport phenomena of the medium. In the calculation of conductivities and corresponding coefficients, we follow the similar methodology as done for the current quark masses but with masses being replaced by the medium-generated masses, i.e., the quasiparticle masses.

It is observed that the heat and charge transport phenomena slightly slow down due to the quasiparticle masses (comparatively heavier) than the current quark masses because of the reduced mobility of carriers. As a result, we see a slightly higher values of σ_{el}, σ_H, κ and κ_H in the case of current quark masses. The ratios of $\sigma_{el}^{\mathrm{BGK}}/\sigma_{el}^{\mathrm{RTA}}$ and $\kappa^{\mathrm{BGK}}/\kappa^{\mathrm{RTA}}$ are observed to be 2.70 [Fig. 5(a)] and 1.39

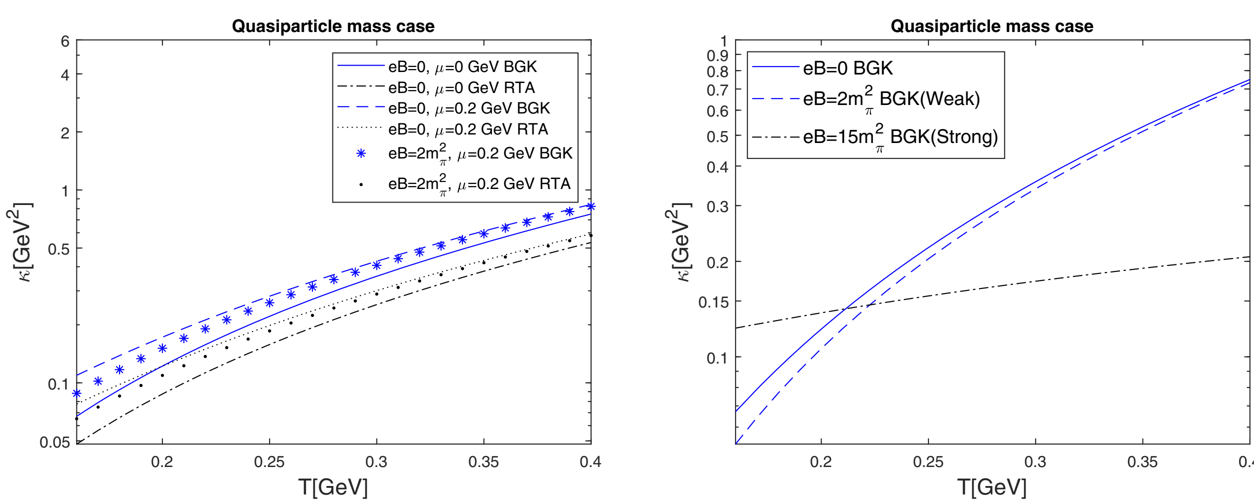

(a) (b)

FIG. 7. The variation of the thermal conductivity (κ) with temperature, (a) comparison with RTA model result (weak magnetic field) and (b) comparison with BGK model result (strong magnetic field).

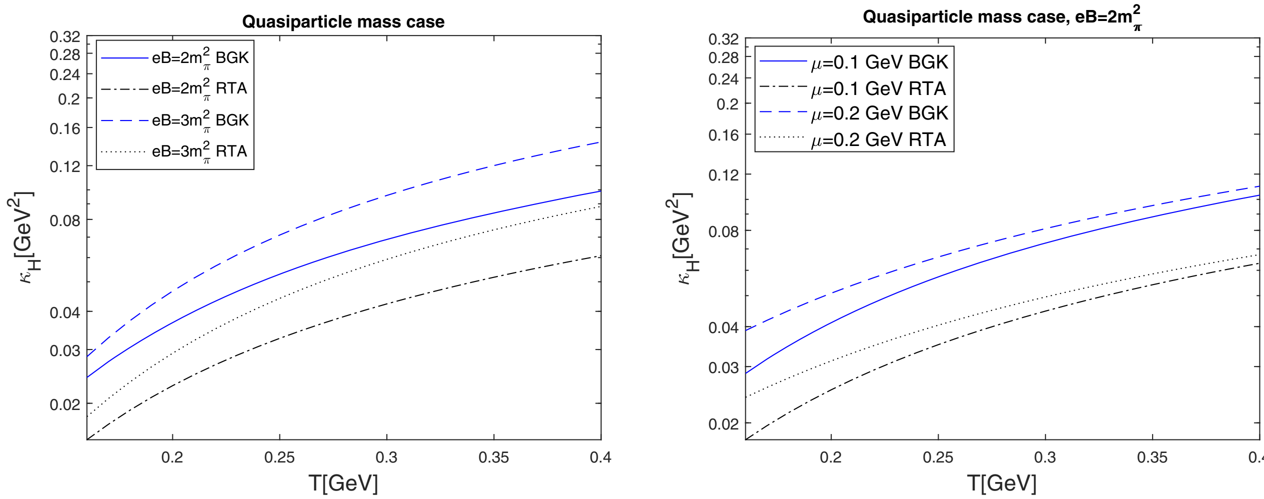

(a) (b)

FIG. 8. The variation of the Hall-type thermal conductivity (κ_H) with temperature, (a) comparison with RTA model result in the presence of weak magnetic field and (b) comparison with RTA model result in the presence of finite chemical potential.

[Fig. 7(a)], respectively. This shows that the collision integral is more sensitive to charge transport, irrespective of quark masses. Figure 5(a) shows the result on electrical conductivity with that of lattice QCD. It is found that the lattice QCD results in Refs. [66,67] are a bit closer to σ_{el} calculated in the quasiparticle model due to the slight reduction in its magnitude as compared to the current quark mass case. Thus, a good agreement with the lattice data is observed when the partons acquire thermal masses.

In the current quark-mass case, the large magnitudes of $\sigma_{\rm el}$ and κ [in BGK (strong) case] are mainly attributed to the phase-space factor ($\sim|q_fB|$), and the relaxation time in the strong magnetic-field limit. The phase-space factor is proportional to $\sim|q_fB|$ and the relaxation time is inversely proportional to the square of the mass [Eq. (60) of Ref. [46]], where the current quark mass is very small. Thus, they overall give an increasing effect to the transport coefficients in the strong magnetic field limit. After the inclusion of the thermal mass, there is a large reduction in the distribution function of particles and the relaxation time as compared to the current quark-mass case. Hence, a decrease in the magnitudes of $\sigma_{\rm el}$ and κ is evidenced and this makes the quasiparticle description of particles a useful tool in taming the large values of transport coefficients in the strong magnetic field.

V. APPLICATIONS

A. Wiedemann-Franz law and Lorenz number

This law states that the ratio of thermal conductivity (κ) to electrical conductivity (σ_{el}) is directly proportional to the

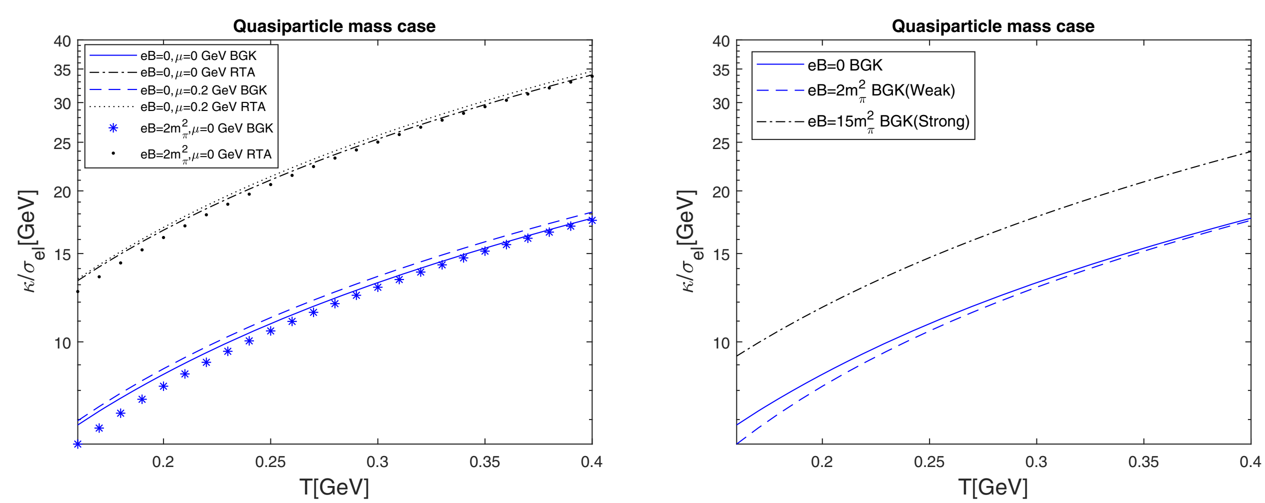

(a) (b)

FIG. 9. The variation of the ratio of the thermal conductivity to the electrical conductivity (κ/σ_{el}) with temperature, (a) comparison with RTA model result (weak magnetic field) and (b) comparison with BGK model result (strong magnetic field).

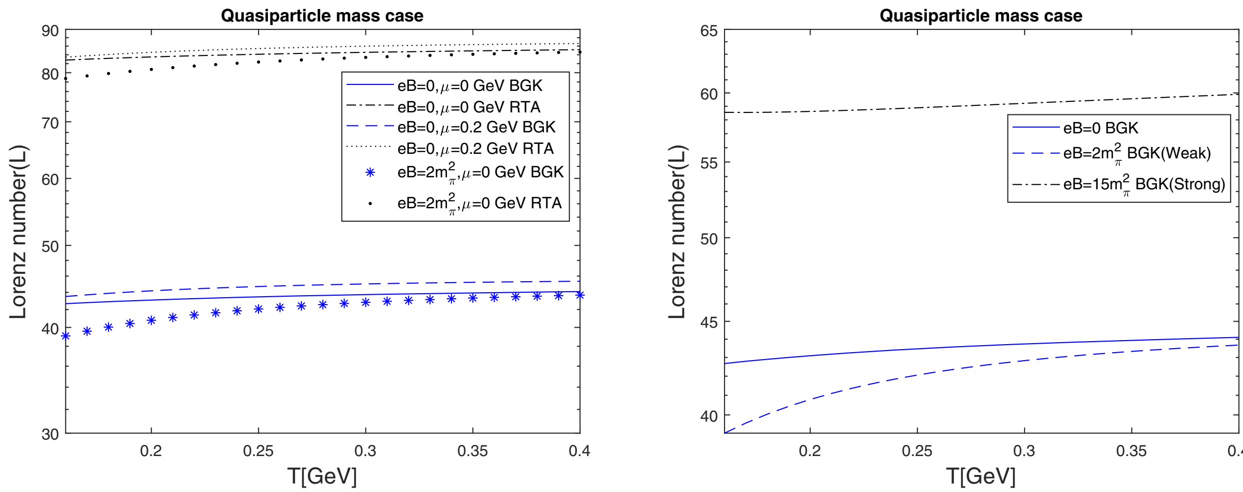

(a) (b)

FIG. 10. The variation of the Lorenz number (L) with temperature, (a) comparison with RTA model result (weak magnetic field) and (b) comparison with BGK model result (strong magnetic field).

temperature (T) through a proportionality factor known as the Lorenz number (L),

$$\frac{\kappa}{\sigma_{el}} = LT. \tag{75}$$

This law indicates the relative behavior of the charge and heat transport phenomena in a medium. In Figs. 9(a) and 9(b), we show the variation of κ/σ_{el} with temperature for different magnetic field strengths and chemical potentials and also compare this result with RTA model (weak magnetic field) and BGK model (strong magnetic field) results, respectively. The same comparison has been done in Fig. 10 [10(a) and 10(b)] for the Lorenz number. It is found that the ratio κ/σ_{el} varies almost linearly with the temperature (Fig. 9), indicating that the heat transport forges ahead of the charge transport as the temperature of the medium increases. For a better understanding of the relative behavior of the aforesaid transport phenomena, the Lorenz number is seen to vary in a monotonically increasing manner for low temperature, indicating the violation of the Wiedemann-Franz law. On the other hand, the Lorenz number saturates at higher temperature (Fig. 10). Figures 9(a) and 10(a) depict the domination of the relaxation collision integral over the BGK collision integral, whereas Figs. 9(b) and 10(b) indicate that the Lorenz number in the strong magnetic field regime prevails over the one in the weak magnetic-field regime.

B. Knudsen number and specific heat

Knudsen number (Ω) is a dimensionless quantity and it is defined as the ratio of the mean-free path (λ) and the characteristic length scale of the medium (l), i.e.,

$$\Omega = \frac{\lambda}{l}. \tag{76}$$

If Ω is less than one (i.e., $\lambda < l$), then we can apply the equilibrium hydrodynamics to this system. So with the help of the Knudsen number, we can predict the local equilibrium of a system. The mean free path λ in Eq. (76) is computed as

$$\lambda = \frac{3\kappa}{VC_v}, \tag{77}$$

where C_v and V represent the specific heat at constant volume and the relative speed, respectively. Specific heat is calculated with the help of the equation given below,

$$C_v = \frac{\partial\epsilon}{\partial T}. \tag{78}$$

Here, ϵ is given in Eq. (41), and we have fixed the value of $V \approx 1$ and $l = 4$ fm.

Figures 11 [11(a) and 11(b)] and 12 [12(a) and 12(b)] show the variations of the Knudsen number and the specific heat with the temperature for different combinations of magnetic field and chemical potential, respectively as well as the comparison with RTA model (weak magnetic field) and BGK model (strong magnetic field) results. Overall, the Knudsen number shows a decreasing trend, whereas specific heat shows an increasing nature with temperature. From the above comparison, we can see that the modified BGK collision term is found to dominate over the RTA collision term, and the BGK model result in the strong magnetic field comes out to be larger than the corresponding weak magnetic field result, which can be understood from the behaviors of κ (Fig. 7) and C_v (Fig. 12) in the

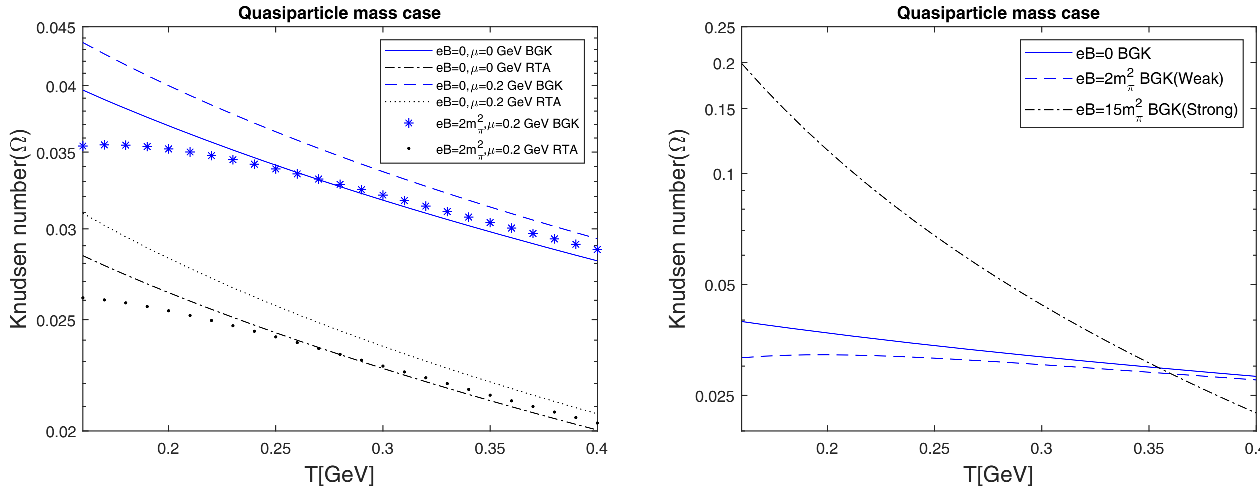

(a) (b)

FIG. 11. The variation of the Knudsen number (Ω) with temperature, (a) comparison with RTA model result (weak magnetic field) and (b) comparison with BGK model result (strong magnetic field).

similar environment. The value of Ω, as seen in Fig. 11 for both the models, is less than unity, which indicates the validity of the system being in local equilibrium even in the presence of both magnetic field and chemical potential.

C. Elliptic flow

The elliptic flow coefficient (v_2) describes the azimuthal anisotropy in the momentum space of produced particles in heavy ion collisions. The elliptic flow is related to the Knudsen number by the following equation [72–74]:

$$v_2 = \frac{v_2^h}{1 + \frac{\Omega}{\Omega_h}}, \tag{79}$$

where v_2^h represents the value of elliptic flow coefficient in the hydrodynamic limit (i.e., $\Omega \to 0$ limit). The value of Ω_h can be calculated by observing the transition between the hydrodynamic regime and the free-streaming particle regime. In our work, we have used $v_2^h \approx 0.1$ and $\Omega_h = 0.7$ and these values are taken from the transport calculation in Ref. [74]. Figure 13 [13(a) and 13(b)] shows the variation of elliptic flow coefficient with the temperature at different combinations of magnetic field and chemical potential as well as the comparison with RTA model (weak magnetic field) and BGK model (strong magnetic field) results. It can be observed that v_2 shows an increasing trend with temperature for different combinations of weak magnetic field and finite chemical potential. From the

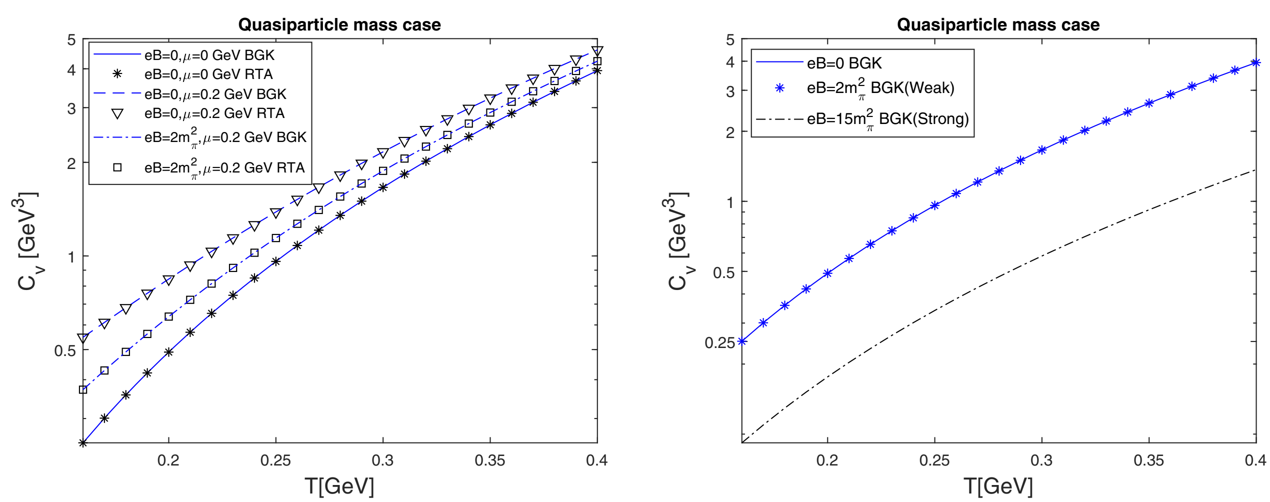

(a) (b)

FIG. 12. The variation of the specific heat (C_v) with temperature, (a) comparison with RTA model result (weak magnetic field) and (b) comparison with BGK model result (strong magnetic field).

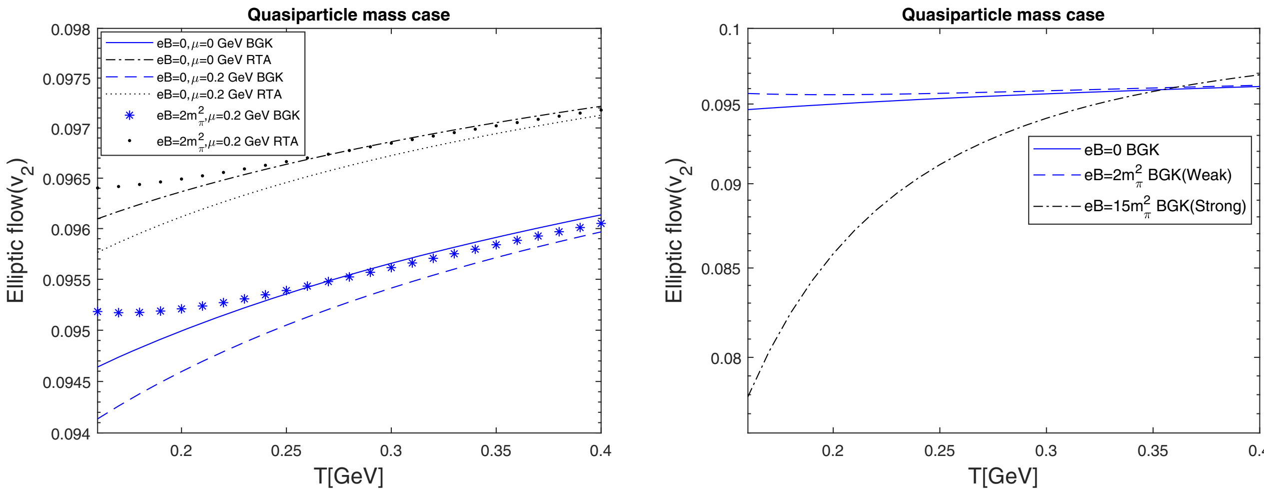

(a) (b)

FIG. 13. The variation of the elliptic flow coefficient (v_2) with temperature, (a) comparison with RTA model result (weak magnetic field) and (b) comparison with BGK model result (strong magnetic field).

above comparison, it is inferred that the RTA collision term dominates over the modified BGK collision term [Fig. 13(a)], and the value of the elliptic flow in BGK model for the strong magnetic field is less than its counterpart in the weak magnetic field [Fig. 13(b)], which can be understood from the behavior of the Knudsen number with temperature as shown in Fig. 11.

VI. SUMMARY

The effects of weak magnetic field and finite chemical potential on a strongly interacting thermal QCD medium have been investigated through different charge and heat transport coefficients. Due to the complicated nature of the collision integral in the Boltzmann transport equation, we considered the problem in a kinetic theory approach with a modified collision integral under the BGK model. The magnetic field was assumed to be weak in comparison to the temperature scale in the system. In the presence of a magnetic field, the transport coefficients lose their isotropic nature and possess different components. Charge and heat transport coefficients, such as electrical conductivity (σ_{el}), Hall conductivity (σ_H), thermal conductivity (κ), and Hall-type thermal conductivity (κ_H) were calculated by solving the relativistic Boltzmann transport equation. We examined how the modified collision integral (BGK model) affects these transport coefficients in comparison to the often used relaxation-type collision integral (RTA model). We also observed how the magnitudes of these coefficients change when we apply the quasiparticle model to the system, where the usual rest masses are being replaced by the medium generated masses. The modified BGK collision integral enhances both the charge transport (σ_{el}, σ_H) and the heat transport (κ, κ_H) coefficients as compared to the RTA collision integral in weak magnetic field. At finite chemical potential, all the charge and heat transport coefficients get enhanced, whereas, with the weak magnetic field, σ_{el} and κ decrease, and σ_H and κ_H increase. The transport coefficients were further used to study the Wiedemann-Franz law, the Lorenz number, the Knudsen number, the specific heat and the elliptic flow. The RTA collision integral dominates over the BGK collision term for the ratio of thermal-to-electrical conductivity (Wiedemann-Franz law). The Lorenz number was seen to increase monotonically with temperature, which indicates the violation of the Wiedemann-Franz law for a thermalized QCD medium in the presence of weak magnetic field. The magnitude of the Knudsen number remains below unity for both BGK and RTA models, which indicates the existence of a local equilibrium for the medium. The elliptic-flow coefficient gets decreased at finite chemical potential, whereas the presence of weak magnetic field increases it. In addition, the elliptic flow coefficient in BGK model was observed to be less than that in RTA model in the presence of a weak magnetic field. Observation also showed that there is a large difference in the magnitudes of elliptic flow in BGK weak and BGK strong magnetic field cases, especially at lower temperatures, whereas this difference gets mitigated at higher temperatures.

ACKNOWLEDGMENTS

One of us (S. R.) acknowledges the Indian Institute of Technology Bombay for the Institute postdoctoral fellowship. S. D. would like to acknowledge the SERB Power Fellowship, SPF/2022/000014 for the support on this work.

APPENDIX A: DERIVATION OF EQUATION (28)

From Eq. (19), we have

$$
\begin{aligned}
f_f &= n_f n_{\mathrm{eq},f}^{-1} f_{\mathrm{eq},f} - \tau_f q\mathbf{E}.\frac{\partial f_{\mathrm{eq},f}}{\partial \mathbf{p}} - \mathbf{\Gamma}.\frac{\partial f_{\mathrm{eq},f}}{\partial \mathbf{p}}, \\
&= n_f n_{\mathrm{eq},f}^{-1} f_{\mathrm{eq},f} - \tau_f qE\frac{\partial f_{\mathrm{eq},f}}{\partial p_x} - \Gamma_x\frac{\partial f_{\mathrm{eq},f}}{\partial p_x} - \Gamma_y\frac{\partial f_{\mathrm{eq},f}}{\partial p_y} - \Gamma_z\frac{\partial f_{\mathrm{eq},f}}{\partial p_z}.
\end{aligned} \tag{A1}
$$

Now, after putting the values of $\frac{\partial f_{\mathrm{eq},f}}{\partial p_x}$, $\frac{\partial f_{\mathrm{eq},f}}{\partial p_y}$, $\frac{\partial f_{\mathrm{eq},f}}{\partial p_z}$ [as given by Eq. (20)], Γ_x, Γ_y, and Γ_z [as given by Eq. (22)] in Eq. (A1), we have

$$
\begin{aligned}
f_f &= n_f n_{\mathrm{eq},f}^{-1} f_{\mathrm{eq},f} - \tau_f qE\{-\beta v_x f_{\mathrm{eq},f}(1-f_{\mathrm{eq},f})\} - \left\{\frac{qE\tau_f(1-\omega_c^2\tau_f^2)}{(1+\omega_c^2\tau_f^2)}\right\}\{-\beta v_x f_{\mathrm{eq},f}(1-f_{\mathrm{eq},f})\} \\
&\quad - \left\{-\frac{2qE\omega_c\tau_f^2}{(1+\omega_c^2\tau_f^2)}\right\}\{-\beta v_y f_{\mathrm{eq},f}(1-f_{\mathrm{eq},f})\}, \\
f_f - n_f n_{\mathrm{eq},f}^{-1} f_{\mathrm{eq},f} &= 2qE\beta v_x\left(\frac{\tau_f}{(1+\omega_c^2\tau_f^2)}\right)f_{\mathrm{eq},f}(1-f_{\mathrm{eq},f}) - 2qE\beta v_y\left(\frac{\omega_c\tau_f^2}{(1+\omega_c^2\tau_f^2)}\right)f_{\mathrm{eq},f}(1-f_{\mathrm{eq},f}).
\end{aligned} \tag{A2}
$$

For a proper treatment of the left-hand side of the above equation, we are considering an infinitesimal perturbation to the equilibrium distribution function: $f_{\mathrm{eq},f} \to f_{\mathrm{eq},f} + \delta f_f$, $\delta f_f \ll f_{\mathrm{eq},f}$ and after linearizing it, we get

$$
\delta f_f - g_f n_{\mathrm{eq},f}^{-1} f_{\mathrm{eq},f}\int_p \delta f_f = 2qE\beta v_x\left(\frac{\tau_f}{(1+\omega_c^2\tau_f^2)}\right)f_{\mathrm{eq},f}(1-f_{\mathrm{eq},f}) - 2qE\beta v_y\left(\frac{\omega_c\tau_f^2}{(1+\omega_c^2\tau_f^2)}\right)f_{\mathrm{eq},f}(1-f_{\mathrm{eq},f}). \tag{A3}
$$

Solving the above equation for δf_f [neglecting the higher-order $\mathcal{O}((\delta f_f)^2)$], we get

$$
\delta f_f = \delta f_f^{(0)} + g_f n_{\mathrm{eq},f}^{-1} f_{\mathrm{eq},f}\int_{p\prime}\delta f_f^{(0)}, \tag{A4}
$$

where

$$
\delta f_f^{(0)} = 2qE\beta v_x\left(\frac{\tau_f}{(1+\omega_c^2\tau_f^2)}\right)f_{\mathrm{eq},f}(1-f_{\mathrm{eq},f}) - 2qE\beta v_y\left(\frac{\omega_c\tau_f^2}{(1+\omega_c^2\tau_f^2)}\right)f_{\mathrm{eq},f}(1-f_{\mathrm{eq},f}). \tag{A5}
$$

Putting it in Eq. (A4), we have

$$
\begin{aligned}
\delta f_f &= \left[2qE\beta v_x\left(\frac{\tau_f}{(1+\omega_c^2\tau_f^2)}\right)f_{\mathrm{eq},f}(1-f_{\mathrm{eq},f}) - 2qE\beta v_y\left(\frac{\omega_c\tau_f^2}{(1+\omega_c^2\tau_f^2)}\right)f_{\mathrm{eq},f}(1-f_{\mathrm{eq},f})\right] \\
&\quad + g_f n_{\mathrm{eq},f}^{-1} f_{\mathrm{eq},f}\int_{p\prime}\left[2qE\beta v_x\left(\frac{\tau_f}{(1+\omega_c^2\tau_f^2)}\right)f_{\mathrm{eq},f}(1-f_{\mathrm{eq},f}) - 2qE\beta v_y\left(\frac{\omega_c\tau_f^2}{(1+\omega_c^2\tau_f^2)}\right)f_{\mathrm{eq},f}(1-f_{\mathrm{eq},f})\right].
\end{aligned} \tag{A6}
$$

Similarly, for antiquarks, we have

$$
\begin{aligned}
\delta\bar{f}_f &= \left[2\bar{q}E\beta v_x\left(\frac{\tau_{\bar{f}}}{(1+\omega_c^2\tau_{\bar{f}}^2)}\right)\bar{f}_{\mathrm{eq},f}(1-\bar{f}_{\mathrm{eq},f}) - 2\bar{q}E\beta v_y\left(\frac{\omega_c\tau_{\bar{f}}^2}{(1+\omega_c^2\tau_{\bar{f}}^2)}\right)\bar{f}_{\mathrm{eq},f}(1-\bar{f}_{\mathrm{eq},f})\right] \\
&\quad + g_f n_{\mathrm{eq},f}^{-1}\bar{f}_{\mathrm{eq},f}\int_{p\prime}\left[2\bar{q}E\beta v_x\left(\frac{\tau_{\bar{f}}}{(1+\omega_c^2\tau_{\bar{f}}^2)}\right)\bar{f}_{\mathrm{eq},f}(1-\bar{f}_{\mathrm{eq},f}) - 2\bar{q}E\beta v_y\left(\frac{\omega_c\tau_{\bar{f}}^2}{(1+\omega_c^2\tau_{\bar{f}}^2)}\right)\bar{f}_{\mathrm{eq},f}(1-\bar{f}_{\mathrm{eq},f})\right].
\end{aligned} \tag{A7}
$$

After substituting the results of Eqs. (A6) and (A7) in Eq. (5), we get

$$J^i = \sum_f g_f q_f \int \frac{d^3p}{(2\pi)^3}\frac{p_\mu}{\omega_f}\left[(A+\bar{A}) + g_f n_{\mathrm{eq},f}^{-1} f_{\mathrm{eq},f}\int_{p'}(A+\bar{A})\right] - \sum_f g_f q_f \int \frac{d^3p}{(2\pi)^3}\frac{p_\mu}{\omega_f}\left[(B+\bar{B}) + g_f n_{\mathrm{eq},f}^{-1} f_{\mathrm{eq},f}\int_{p'}(B+\bar{B})\right], \tag{A8}$$

where

$$A = 2qE\beta v_x\left(\frac{\tau_f}{(1+\omega_c^2\tau_f^2)}\right) f_{\mathrm{eq},f}(1-f_{\mathrm{eq},f}), \tag{A9}$$

$$B = 2qE\beta v_y\left(\frac{\omega_c\tau_f^2}{(1+\omega_c^2\tau_f^2)}\right) f_{\mathrm{eq},f}(1-f_{\mathrm{eq},f}), \tag{A10}$$

$$\bar{A} = 2\bar{q}E\beta v_x\left(\frac{\tau_{\bar{f}}}{(1+\omega_c^2\tau_{\bar{f}}^2)}\right) \bar{f}_{\mathrm{eq},f}(1-\bar{f}_{\mathrm{eq},f}), \tag{A11}$$

$$\bar{B} = 2\bar{q}E\beta v_y\left(\frac{\omega_c\tau_{\bar{f}}^2}{(1+\omega_c^2\tau_{\bar{f}}^2)}\right) \bar{f}_{\mathrm{eq},f}(1-\bar{f}_{\mathrm{eq},f}). \tag{A12}$$

Now recalling Eq. (7),

$$J^i = \sigma^{ij}E_j = (\sigma_{el}\delta^{ij} + \sigma_H\epsilon^{ij})E_j \tag{A13}$$

and comparing Eq. (A8) with this equation, we get the final expressions of electrical conductivity (σ_{el}) and Hall conductivity (σ_H) as given in Eqs. (30) and (31), respectively.

APPENDIX B: DERIVATION OF EQUATION (64)

After substituting the values of $\frac{\partial f_{\mathrm{eq},f}}{\partial p_x}, \frac{\partial f_{\mathrm{eq},f}}{\partial p_y}, \frac{\partial f_{\mathrm{eq},f}}{\partial p_z}$ [as given by Eq. (20)], Γ_x, Γ_y, and Γ_z (as given by equations (57), (58), and (59), respectively) in Eq. (A1), we get

$$\begin{aligned} f_f =& n_f n_{\mathrm{eq},f}^{-1} f_{\mathrm{eq},f} - \tau_f qE\{-\beta v_x f_{\mathrm{eq},f}(1-f_{\mathrm{eq},f})\} - \left\{qE\tau_f\frac{(1-\omega_c^2\tau_f^2)}{(1+\omega_c^2\tau_f^2)} - \frac{\tau_f}{(1+\omega_c^2\tau_f^2)}\frac{(\omega_f-h_f)}{T}\left(\partial^x T - \frac{T}{nh_f}\partial^x P\right)\right.\\ &\left.- \frac{\omega_c\tau_f^2}{(1+\omega_c^2\tau_f^2)}\frac{(\omega_f-h_f)}{T}\left(\partial^y T - \frac{T}{nh_f}\partial^y P\right)\right\}\{-\beta v_x f_{\mathrm{eq},f}(1-f_{\mathrm{eq},f})\} - \left\{-\frac{2qE\omega_c\tau_f^2}{(1+\omega_c^2\tau_f^2)} - \frac{\tau_f}{(1+\omega_c^2\tau_f^2)}\right.\\ &\left.\times\frac{(\omega_f-h_f)}{T}\left(\partial^y T - \frac{T}{nh_f}\partial^y P\right) + \frac{\omega_c\tau_f^2}{(1+\omega_c^2\tau_f^2)}\frac{(\omega_f-h_f)}{T}\left(\partial^x T - \frac{T}{nh_f}\partial^x P\right)\right\}\{-\beta v_y f_{\mathrm{eq},f}(1-f_{\mathrm{eq},f})\}, \end{aligned}$$

$$\begin{aligned} f_f - n_f n_{\mathrm{eq},f}^{-1} f_{\mathrm{eq},f} =& \frac{2qE\tau_f v_x\beta}{(1+\omega_c^2\tau_f^2)} f_{\mathrm{eq},f}(1-f_{\mathrm{eq},f}) - \frac{2qE\omega_c\tau_f^2 v_y\beta}{(1+\omega_c^2\tau_f^2)} f_{\mathrm{eq},f}(1-f_{\mathrm{eq},f}) - \beta f_{\mathrm{eq},f}(1-f_{\mathrm{eq},f})\frac{\tau_f}{(1+\omega_c^2\tau_f^2)}\\ &\times\frac{(\omega_f-h_f)}{T}\left[v_x\left(\partial^x T - \frac{T}{nh_f}\partial^x P\right) + v_y\left(\partial^y T - \frac{T}{nh_f}\partial^y P\right)\right]\\ &- \beta f_{\mathrm{eq},f}(1-f_{\mathrm{eq},f})\frac{\omega_c\tau_f^2}{(1+\omega_c^2\tau_f^2)}\frac{(\omega_f-h_f)}{T}\left[v_x\left(\partial^y T - \frac{T}{nh_f}\partial^y P\right) - v_y\left(\partial^x T - \frac{T}{nh_f}\partial^x P\right)\right]. \end{aligned} \tag{B1}$$

Following the previous steps [as done in Eqs. (A3) and (A4)], we have

$$\delta f_f^{(0)} = \frac{2qE\tau_f v_x\beta}{(1+\omega_c^2\tau_f^2)} f_{\mathrm{eq},f}(1-f_{\mathrm{eq},f}) - \frac{2qE\omega_c\tau_f^2 v_y\beta}{(1+\omega_c^2\tau_f^2)} f_{\mathrm{eq},f}(1-f_{\mathrm{eq},f}) - \beta f_{\mathrm{eq},f}(1-f_{\mathrm{eq},f})\frac{\tau_f}{(1+\omega_c^2\tau_f^2)}\frac{(\omega_f-h_f)}{T} \times\left[v_x\left(\partial^x T - \frac{T}{nh_f}\partial^x P\right) + v_y\left(\partial^y T - \frac{T}{nh_f}\partial^y P\right)\right] - \beta f_{\mathrm{eq},f}(1-f_{\mathrm{eq},f})\frac{\omega_c\tau_f^2}{(1+\omega_c^2\tau_f^2)}\frac{(\omega_f-h_f)}{T}\left[v_x\left(\partial^y T - \frac{T}{nh_f}\partial^y P\right) - v_y\left(\partial^x T - \frac{T}{nh_f}\partial^x P\right)\right], \tag{B2}$$

$$\delta f_f = \frac{2qE\tau_f v_x\beta}{(1+\omega_c^2\tau_f^2)} f_{\mathrm{eq},f}(1-f_{\mathrm{eq},f}) - \frac{2qE\omega_c\tau_f^2 v_y\beta}{(1+\omega_c^2\tau_f^2)} f_{\mathrm{eq},f}(1-f_{\mathrm{eq},f}) - \beta f_{\mathrm{eq},f}(1-f_{\mathrm{eq},f})\frac{\tau_f}{(1+\omega_c^2\tau_f^2)}\frac{(\omega_f-h_f)}{T} \times\left[v_x\left(\partial^x T - \frac{T}{nh_f}\partial^x P\right) + v_y\left(\partial^y T - \frac{T}{nh_f}\partial^y P\right)\right] - \beta f_{\mathrm{eq},f}(1-f_{\mathrm{eq},f})\frac{\omega_c\tau_f^2}{(1+\omega_c^2\tau_f^2)}\frac{(\omega_f-h_f)}{T} \times\left[v_x\left(\partial^y T - \frac{T}{nh_f}\partial^y P\right) - v_y\left(\partial^x T - \frac{T}{nh_f}\partial^x P\right)\right] + g_f n_{\mathrm{eq},f}^{-1} f_{\mathrm{eq},f}\int_{p\prime}\left[\frac{2qE\tau_f v_x\beta}{(1+\omega_c^2\tau_f^2)} f_{\mathrm{eq},f}(1-f_{\mathrm{eq},f}) - \frac{2qE\omega_c\tau_f^2 v_y\beta}{(1+\omega_c^2\tau_f^2)} f_{\mathrm{eq},f}(1-f_{\mathrm{eq},f}) - \beta f_{\mathrm{eq},f}(1-f_{\mathrm{eq},f})\frac{\tau_f}{(1+\omega_c^2\tau_f^2)} \times\frac{(\omega_f-h_f)}{T}\left[v_x\left(\partial^x T - \frac{T}{nh_f}\partial^x P\right) + v_y\left(\partial^y T - \frac{T}{nh_f}\partial^y P\right)\right] - \beta f_{\mathrm{eq},f}(1-f_{\mathrm{eq},f})\frac{\omega_c\tau_f^2}{(1+\omega_c^2\tau_f^2)}\frac{(\omega_f-h_f)}{T}\left[v_x\left(\partial^y T - \frac{T}{nh_f}\partial^y P\right) - v_y\left(\partial^x T - \frac{T}{nh_f}\partial^x P\right)\right]\right], \tag{B3}$$

and

$$\delta\bar{f}_f = \frac{2qE\tau_{\bar{f}} v_x\beta}{(1+\omega_c^2\tau_{\bar{f}}^2)} \bar{f}_{\mathrm{eq},f}(1-\bar{f}_{\mathrm{eq},f}) - \frac{2qE\omega_c\tau_{\bar{f}}^2 v_y\beta}{(1+\omega_c^2\tau_{\bar{f}}^2)} \bar{f}_{\mathrm{eq},f}(1-\bar{f}_{\mathrm{eq},f}) - \beta\bar{f}_{\mathrm{eq},f}(1-\bar{f}_{\mathrm{eq},f})\frac{\tau_{\bar{f}}}{(1+\omega_c^2\tau_{\bar{f}}^2)}\frac{(\omega_f-h_{\bar{f}})}{T} \times\left[v_x\left(\partial^x T - \frac{T}{nh_f}\partial^x P\right) + v_y\left(\partial^y T - \frac{T}{nh_f}\partial^y P\right)\right] - \beta\bar{f}_{\mathrm{eq},f}(1-\bar{f}_{\mathrm{eq},f})\frac{\omega_c\tau_{\bar{f}}^2}{(1+\omega_c^2\tau_{\bar{f}}^2)}\frac{(\omega_f-h_{\bar{f}})}{T} \times\left[v_x\left(\partial^y T - \frac{T}{nh_f}\partial^y P\right) - v_y\left(\partial^x T - \frac{T}{nh_f}\partial^x P\right)\right] + g_f n_{\mathrm{eq},f}^{-1}\bar{f}_{\mathrm{eq},f}\int_{p\prime}\left[\frac{2qE\tau_{\bar{f}} v_x\beta}{(1+\omega_c^2\tau_{\bar{f}}^2)} \bar{f}_{\mathrm{eq},f}(1-\bar{f}_{\mathrm{eq},f}) - \frac{2qE\omega_c\tau_{\bar{f}}^2 v_y\beta}{(1+\omega_c^2\tau_{\bar{f}}^2)} \bar{f}_{\mathrm{eq},f}(1-\bar{f}_{\mathrm{eq},f}) - \beta\bar{f}_{\mathrm{eq},f}(1-\bar{f}_{\mathrm{eq},f})\frac{\tau_{\bar{f}}}{(1+\omega_c^2\tau_{\bar{f}}^2)} \times\frac{(\omega_f-h_{\bar{f}})}{T}\left[v_x\left(\partial^x T - \frac{T}{nh_f}\partial^x P\right) + v_y\left(\partial^y T - \frac{T}{nh_f}\partial^y P\right)\right] - \beta\bar{f}_{\mathrm{eq},f}(1-\bar{f}_{\mathrm{eq},f})\frac{\omega_c\tau_{\bar{f}}^2}{(1+\omega_c^2\tau_{\bar{f}}^2)}\frac{(\omega_f-h_{\bar{f}})}{T}\left[v_x\left(\partial^y T - \frac{T}{nh_f}\partial^y P\right) - v_y\left(\partial^x T - \frac{T}{nh_f}\partial^x P\right)\right]\right]. \tag{B4}$$

After putting the results of Eqs. (B3) and (B4) in Eq. (46), we get

$$Q^i = \sum_f g_f\int\frac{d^3p}{(2\pi)^3}\frac{p^i}{\omega_f}\left[(\omega_f-h_f)[(2qEv_x\beta A - 2qEv_y\beta B - \beta^2 C - \beta^2 D) + g_f n_{\mathrm{eq},f}^{-1} f_{\mathrm{eq},f}\int_{p\prime}(2qEv_x\beta A - 2qEv_y\beta B - \beta^2 C - \beta^2 D)] + (\omega_f - h_{\bar{f}})[(2qEv_x\beta\bar{A} - 2qEv_y\beta\bar{B} - \beta^2\bar{C} - \beta^2\bar{D}) + g_f n_{\mathrm{eq},f}^{-1} f_{\mathrm{eq},f}\int_{p\prime}(2qEv_x\beta\bar{A} - 2qEv_y\beta\bar{B} - \beta^2\bar{C} - \beta^2\bar{D})]\right], \tag{B5}$$

where

$$A = \frac{\tau_f}{(1+\omega_c^2\tau_f^2)} f_{\mathrm{eq},f}(1-f_{\mathrm{eq},f}), \tag{B6}$$

$$B = \frac{\omega_c\tau_f^2}{(1+\omega_c^2\tau_f^2)} f_{\mathrm{eq},f}(1-f_{\mathrm{eq},f}), \tag{B7}$$

$$C = \frac{\tau_f}{(1+\omega_c^2\tau_f^2)}(\omega_f - h_f) f_{\mathrm{eq},f}(1-f_{\mathrm{eq},f})\left[v_x\left(\partial^x T - \frac{T}{nh_f}\partial^x P\right) + v_y\left(\partial^y T - \frac{T}{nh_f}\partial^y P\right)\right], \tag{B8}$$

$$D = \frac{\omega_c\tau_f^2}{(1+\omega_c^2\tau_f^2)}(\omega_f - h_f) f_{\mathrm{eq},f}(1-f_{\mathrm{eq},f})\left[v_x\left(\partial^y T - \frac{T}{nh_f}\partial^y P\right) - v_y\left(\partial^x T - \frac{T}{nh_f}\partial^x P\right)\right], \tag{B9}$$

$$\bar{A} = \frac{\tau_{\bar{f}}}{(1+\omega_c^2\tau_{\bar{f}}^2)} \bar{f}_{\mathrm{eq},f}(1-\bar{f}_{\mathrm{eq},f}), \tag{B10}$$

$$\bar{B} = \frac{\omega_c\tau_{\bar{f}}^2}{(1+\omega_c^2\tau_{\bar{f}}^2)} \bar{f}_{\mathrm{eq},f}(1-\bar{f}_{\mathrm{eq},f}), \tag{B11}$$

$$\bar{C} = \frac{\tau_{\bar{f}}}{(1+\omega_c^2\tau_{\bar{f}}^2)}(\omega_f - h_{\bar{f}}) \bar{f}_{\mathrm{eq},f}(1-\bar{f}_{\mathrm{eq},f})\left[v_x\left(\partial^x T - \frac{T}{nh_f}\partial^x P\right) + v_y\left(\partial^y T - \frac{T}{nh_f}\partial^y P\right)\right], \tag{B12}$$

$$\bar{D} = \frac{\omega_c\tau_{\bar{f}}^2}{(1+\omega_c^2\tau_{\bar{f}}^2)}(\omega_f - h_{\bar{f}}) \bar{f}_{\mathrm{eq},f}(1-\bar{f}_{\mathrm{eq},f})\left[v_x\left(\partial^y T - \frac{T}{nh_f}\partial^y P\right) - v_y\left(\partial^x T - \frac{T}{nh_f}\partial^x P\right)\right]. \tag{B13}$$

Now recalling Eq. (53),

$$Q^i = -(\kappa\delta^{ij} + \kappa_H\epsilon^{ij})\left[\partial_j T - \frac{T}{(n_{\mathrm{eq},f}h_f)}\partial_j P\right] \tag{B14}$$

and comparing Eq. (B5) with this equation, we get the final expressions of thermal conductivity (κ) and Hall-type thermal conductivity (κ_H) as given in Eqs. (66) and (67), respectively.

[1] Skokov, A. Yu Illarionov, and V. D. Toneev, Estimate of the magnetic field strength in heavy-ion collisions, Int. J. Mod. Phys. A **24**, 5925 (2009).

[2] Adam Bzdak and Vladimir Skokov, Event-by-event fluctuations of magnetic and electric fields in heavy ion collisions, Phys. Lett. B **710**, 171 (2012).

[3] Kenji Fukushima, Dmitri E. Kharzeev, and Harmen J. Warringa, chiral magnetic effect, Phys. Rev. D **78**, 074033 (2008).

[4] Dmitri E. Kharzeev, Larry D. McLerran, and Harmen J. Warringa, The effects of topological charge change in heavy ion collisions: "Event by event P and *CP* violation", Nucl. Phys. **A803**, 227 (2008).

[5] V. Braguta, M. N. Chernodub, V. A. Goy, K. Landsteiner, A. V. Molochkov, and M. I. Polikarpov, Temperature dependence of the axial magnetic effect in two-color quenched QCD, Phys. Rev. D **89**, 074510 (2014).

[6] Maxim N. Chernodub, Alberto Cortijo, Adolfo G. Grushin, Karl Landsteiner, and Mar'ıa A. H. Vozmediano, Condensed matter realization of the axial magnetic effect, Phys. Rev. B **89**, 081407 (2014).

[7] V. P. Gusynin, V. A. Miransky, and I. A. Shovkovy, Catalysis of Dynamical Flavor Symmetry Breaking by A Magnetic Field in 2 + 1 Dimensions, Phys. Rev. Lett. **73**, 3499 (1994).

[8] D.-S. Lee, Chung Ngoc Leung, and Y. J. Ng, Chiral symmetry breaking in a uniform external magnetic field, Phys. Rev. D **55**, 6504 (1997).

[9] Dmitri E. Kharzeev, The chiral magnetic effect and anomaly-induced transport, Prog. Part. Nucl. Phys. **75**, 133 (2014).

[10] Daisuke Satow, Nonlinear electromagnetic response in quark-gluon plasma, Phys. Rev. D **90**, 034018 (2014).
[11] Dmitri E. Kharzeev and Dam T. Son, Testing the Chiral Magnetic and Chiral Vortical Effects in Heavy Ion Collisions, Phys. Rev. Lett. **106**, 062301 (2011).
[12] Shi Pu, Shang-Yu Wu, and Di-Lun Yang, Chiral Hall effect and chiral electric waves, Phys. Rev. D **91**, 025011 (2015).
[13] Sh. Fayazbakhsh and N. Sadooghi, Weak decay constant of neutral pions in a hot and magnetized quark matter, Phys. Rev. D **88**, 065030 (2013).
[14] Sh. Fayazbakhsh, S. Sadeghian, and N. Sadooghi, Properties of neutral mesons in a hot and magnetized quark matter, Phys. Rev. D **86**, 085042 (2012).
[15] N. Sadooghi and F. Taghinavaz, Magnetized plasminos in cold and hot QED plasmas, Phys. Rev. D **92**, 025006 (2015).
[16] Hendrik van Hees, Charles Gale, and Ralf Rapp, Thermal photons and collective flow at energies available at the BNL Relativistic Heavy-Ion Collider, Phys. Rev. C **84**, 054906 (2011).
[17] Chun Shen, Ulrich Heinz, Jean-Francois Paquet, and Charles Gale, Thermal photons as a quark-gluon plasma thermometer reexamined, Phys. Rev. C **89**, 044910 (2014).
[18] Kirill Tuchin, Magnetic contribution to dilepton production in heavy-ion collisions, Phys. Rev. C **88**, 024910 (2013).
[19] Shubhalaxmi Rath and Binoy Krishna Patra, One-loop QCD thermodynamics in a strong homogeneous and static magnetic field, J. High Energy Phys. 12 (2017) 098.
[20] Aritra Bandyopadhyay, Bithika Karmakar, Najmul Haque, and Munshi G. Mustafa, Pressure of a weakly magnetized hot and dense deconfined QCD matter in one-loop hard-thermal-loop perturbation theory, Phys. Rev. D **100**, 034031 (2019).
[21] Shubhalaxmi Rath and Binoy Krishna Patra, Thermomagnetic properties and Bjorken expansion of hot QCD matter in a strong magnetic field, Eur. Phys. J. A **55**, 1 (2019).
[22] Bithika Karmakar, Ritesh Ghosh, Aritra Bandyopadhyay, Najmul Haque, and Munshi G. Mustafa, Anisotropic pressure of deconfined QCD matter in presence of strong magnetic field within one-loop approximation, Phys. Rev. D **99**, 094002 (2019).
[23] Kenji Fukushima, Koichi Hattori, Ho-Ung Yee, and Yi Yin, Heavy quark diffusion in strong magnetic fields at weak coupling and implications for elliptic flow, Phys. Rev. D **93**, 074028 (2016).
[24] K. K. Gowthama, Manu Kurian, and Vinod Chandra, Electromagnetic response of hot QCD medium in the presence of background time-varying fields, Phys. Rev. D **104**, 094037 (2021).
[25] K. K. Gowthama, Manu Kurian, and Vinod Chandra, Thermal and thermoelectric responses of hot QCD medium in time-varying magnetic fields, Phys. Rev. D **106**, 034008 (2022).
[26] Victor Roy, Shi Pu, Luciano Rezzolla, and Dirk Rischke, Analytic Bjorken flow in one-dimensional relativistic magnetohydrodynamics, Phys. Lett. B **750**, 45 (2015).
[27] Gabriele Inghirami, Luca Del Zanna, Andrea Beraudo, Mohsen Haddadi Moghaddam, Francesco Becattini, and Marcus Bleicher, Numerical magneto-hydrodynamics for relativistic nuclear collisions, Eur. Phys. J. C **76**, 1 (2016).
[28] Joseph I. Kapusta and Charles Gale, *Finite-Temperature Field Theory: Principles and Applications* (Cambridge University Press, Cambridge, England, 2006).
[29] Seung-il Nam, Electrical conductivity of quark matter at finite T under external magnetic field, Phys. Rev. D **86**, 033014 (2012).
[30] Koichi Hattori and Daisuke Satow, Electrical conductivity of quark-gluon plasma in strong magnetic fields, Phys. Rev. D **94**, 114032 (2016).
[31] P. V. Buividovich, Maxim N. Chernodub, D. E. Kharzeev, T. Kalaydzhyan, E. V. Luschevskaya, and M. I. Polikarpov, Magnetic-Field-Induced Insulator-Conductor Transition in SU(2) Quenched Lattice Gauge Theory, Phys. Rev. Lett. **105**, 132001 (2010).
[32] Manu Kurian and Vinod Chandra, Effective description of hot QCD medium in strong magnetic field and longitudinal conductivity, Phys. Rev. D **96**, 114026 (2017).
[33] Manu Kurian, Sukanya Mitra, Snigdha Ghosh, and Vinod Chandra, Transport coefficients of hot magnetized QCD matter beyond the lowest Landau level approximation, Eur. Phys. J. C **79**, 1 (2019).
[34] Shubhalaxmi Rath and Binoy Krishna Patra, Revisit to electrical and thermal conductivities, Lorenz and Knudsen numbers in thermal QCD in a strong magnetic field, Phys. Rev. D **100**, 016009 (2019).
[35] Azwinndini Muronga, Relativistic dynamics of non-ideal fluids: Viscous and heat-conducting fluids. II. Transport properties and microscopic description of relativistic nuclear matter, Phys. Rev. C **76**, 014910 (2007).
[36] A. Puglisi, S. Plumari, and V. Greco, Electric Conductivity from the solution of the relativistic Boltzmann equation, Phys. Rev. D **90**, 114009 (2014).
[37] Lata Thakur, P. K. Srivastava, Guru Prakash Kadam, Manu George, and Hiranmaya Mishra, Shear viscosity η to electrical conductivity σ el ratio for an anisotropic QGP, Phys. Rev. D **95**, 096009 (2017).
[38] Shigehiro Yasui and Sho Ozaki, Transport coefficients from the QCD Kondo effect, Phys. Rev. D **96**, 114027 (2017).
[39] Sukanya Mitra and Vinod Chandra, Thermal relaxation, electrical conductivity, and charge diffusion in a hot QCD medium, Phys. Rev. D **94**, 034025 (2016).
[40] Sukanya Mitra and Vinod Chandra, Transport coefficients of a hot QCD medium and their relative significance in heavy-ion collisions, Phys. Rev. D **96**, 094003 (2017).
[41] Moritz Greif, Ioannis Bouras, Carsten Greiner, and Zhe Xu, Electric conductivity of the quark-gluon plasma investigated using a perturbative QCD based parton cascade, Phys. Rev. D **90**, 094014 (2014).
[42] Bohao Feng, Electric conductivity and Hall conductivity of the QGP in a magnetic field, Phys. Rev. D **96**, 036009 (2017).
[43] Gabriel S. Denicol, Xu-Guang Huang, Etele Moln'ar, Gustavo M. Monteiro, Harri Niemi, Jorge Noronha, Dirk H. Rischke, and Qun Wang, Nonresistive dissipative magnetohydrodynamics from the Boltzmann equation in the 14-moment approximation, Phys. Rev. D **98**, 076009 (2018).
[44] Shubhalaxmi Rath and Sadhana Dash, Effects of weak magnetic field and finite chemical potential on the transport of charge and heat in hot QCD matter, Eur. Phys. J. A **59**, 25 (2023).

[45] Prabhu Lal Bhatnagar, Eugene P. Gross, and Max Krook, A model for collision processes in gases. I. Small amplitude processes in charged and neutral one-component systems, Phys. Rev. **94**, 511 (1954).

[46] Salman Ahamad Khan and Binoy Krishna Patra, Cumulative effects of collision integral, strong magnetic field, and quasiparticle description on charge and heat transport in a thermal QCD medium, Phys. Rev. D **104**, 054024 (2021).

[47] Bjoern Schenke, Michael Strickland, Carsten Greiner, and Markus H. Thoma, Model of the effect of collisions on QCD plasma instabilities, Phys. Rev. D **73**, 125004 (2006).

[48] V. Goloviznin and Helmut Satz, The refractive properties of the gluon plasma in SU(2) gauge theory, Z. Phys. C Part. Fields **57**, 671 (1993).

[49] Andr'e Peshier, B. Kämpfer, O. P. Pavlenko, and G. Soff, Massive quasiparticle model of the SU(3) gluon plasma, Phys. Rev. D **54**, 2399 (1996).

[50] Kenji Fukushima, Chiral effective model with the Polyakov loop, Phys. Lett. B **591**, 277 (2004).

[51] Sanjay K. Ghosh, Tamal K. Mukherjee, Munshi G. Mustafa, and Rajarshi Ray, Susceptibilities and speed of sound from the Polyakov-Nambu-Jona-Lasinio model, Phys. Rev. D **73**, 114007 (2006).

[52] Hiroaki Abuki and Kenji Fukushima, Gauge dynamics in the PNJL model: Color neutrality and Casimir scaling, Phys. Lett. B **676**, 57 (2009).

[53] Vishnu M. Bannur, Quasi-particle model for QGP with nonzero densities, J. High Energy Phys. 09 (2007) 046.

[54] Vishnu M. Bannur, Self-consistent quasiparticle model for quark-gluon plasma, Phys. Rev. C **75**, 044905 (2007).

[55] Shubhalaxmi Rath and Binoy Krishna Patra, Momentum and its affiliated transport coefficients for hot QCD matter in a strong magnetic field, Phys. Rev. D **102**, 036011 (2020).

[56] Shubhalaxmi Rath and Binoy Krishna Patra, Viscous properties of hot and dense QCD matter in the presence of a magnetic field, Eur. Phys. J. C **81**, 1 (2021).

[57] Nan Su and Konrad Tywoniuk, Massless Mode and Positivity Violation in Hot QCD, Phys. Rev. Lett. **114**, 161601 (2015).

[58] Wojciech Florkowski, Radoslaw Ryblewski, Nan Su, and Konrad Tywoniuk, Transport coefficients of the Gribov-Zwanziger plasma, Phys. Rev. C **94**, 044904 (2016).

[59] A. Hosoya and Keijo Kajantie, Transport coefficients of QCD matter, Nucl. Phys. **B250**, 666 (1985).

[60] Alejandro Ayala, C. A. Dominguez, Saul Hernandez-Ortiz, L. A. Hernandez, M. Loewe, D. Manreza Paret, and R. Zamora, Thermomagnetic evolution of the QCD strong coupling, Phys. Rev. D **98**, 031501 (2018).

[61] Arpan Das, Hiranmaya Mishra, and Ranjita K. Mohapatra, Electrical conductivity and Hall conductivity of a hot and dense quark gluon plasma in a magnetic field: A quasiparticle approach, Phys. Rev. D **101**, 034027 (2020).

[62] Arpan Das, Hiranmaya Mishra, and Ranjita K. Mohapatra, Electrical conductivity and Hall conductivity of a hot and dense hadron gas in a magnetic field: A relaxation time approach, Phys. Rev. D **99**, 094031 (2019).

[63] Aritra Bandyopadhyay, Sabyasachi Ghosh, Ricardo L. S. Farias, Jayanta Dey, and Gastão Krein, Anisotropic electrical conductivity of magnetized hot quark matter, Phys. Rev. D **102**, 114015 (2020).

[64] Lata Thakur and P. K. Srivastava, Electrical conductivity of a hot and dense QGP medium in a magnetic field, Phys. Rev. D **100**, 076016 (2019).

[65] M. Greif, F. Reining, I. Bouras, G. S. Denicol, Z. Xu, and C. Greiner, Heat conductivity in relativistic systems investigated using a partonic cascade, Phys. Rev. E **87**, 033019 (2013).

[66] G. Aarts, C. Allton, A. Amato, P. Giudice, S. Hands, and J.-I. Skullerud, Electrical conductivity and charge diffusion in thermal QCD from the lattice, J. High Energy Phys. 02 (2015) 186.

[67] A. Amato, G. Aarts, C. Allton, P. Giudice, S. Hands, and J.-I. Skullerud, Electrical Conductivity of the Quark-Gluon Plasma Across the Deconfinement Transition, Phys. Rev. Lett. **111**, 172001 (2013).

[68] H.-T. Ding, O. Kaczmarek, and F. Meyer, Vector spectral functions and transport properties in quenched QCD, Proc. Sci. LATTICE2014 (**2015**) 216.

[69] Eric Braaten and Robert D. Pisarski, Simple effective Lagrangian for hard thermal loops, Phys. Rev. D **45**, R1827 (1992).

[70] A. Peshier, B. Kämpfer, and G. Soff, From QCD lattice calculations to the equation of state of quark matter, Phys. Rev. D **66**, 094003 (2002).

[71] M. Le Bellac, *Thermal Field Theory*, Cambridge Monographs on Mathematical Physics (Cambridge University Press, Cambridge, England, 2011).

[72] Rajeev S. Bhalerao, Jean-Paul Blaizot, Nicolas Borghini, and Jean-Yves Ollitrault, Elliptic flow and incomplete equilibration at RHIC, Phys. Lett. B **627**, 49 (2005).

[73] Hans-Joachim Drescher, Adrian Dumitru, Clément Gombeaud, and Jean-Yves Ollitrault, Centrality dependence of elliptic flow, the hydrodynamic limit, and the viscosity of hot QCD, Phys. Rev. C **76**, 024905 (2007).

[74] Clément Gombeaud and Jean-Yves Ollitrault, Covariant transport theory approach to elliptic flow in relativistic heavy ion collision, Phys. Rev. C **77**, 054904 (2008).